



TKN

Telecommunication
Networks Group

Technical University Berlin

Telecommunication Networks Group

Dynamic OFDM-FDMA systems under
realistic assumptions: On the influence of
channel knowlegde and inband signaling

James Gross, Stefan Valentin, Randy Vu

{ gross, valentin, vu }@tkn.tu-berlin.de

Berlin, October 2004

TKN Technical Report TKN-04-015

TKN Technical Reports Series

Editor: Prof. Dr.-Ing. Adam Wolisz

Abstract

Wireless OFDM systems offer the opportunity to transmit data simultaneously on the down-link of a cell to different wireless terminals by assigning different sets of subcarriers to different terminals. Due to the time- and frequency varying nature of subcarrier gains doing this *dynamically* has been shown to be beneficial in terms of various transmission metrics, i.e. average throughput, consumed power etc. . The potential of these dynamic subcarrier assignment schemes depends on two requirements. First, the access point has to “know” all subcarrier gains of all terminals in order to decide which terminals will receive which subcarrier. Second, after this decision has been made the terminals have to be informed of their assigned subcarrier sets. This task might be solved by a signaling system. So far, recent studies have always just assumed the existence of these two requirements without any cost. In this report we study the impact of explicitly implementing these two tasks in a dynamic assignment system, answering the question: which degree of advantage remains after considering realistic channel knowledge and an implemented signaling system.

Contents

1	Introduction	2
2	System Model	4
2.1	Considered Scenario and Environment	4
2.2	Physical Layer Model	5
2.3	Medium Access Control Layer	8
2.3.1	MAC Timing and Frame Elements	9
2.3.2	The Signaling System	10
2.3.3	Subcarrier Gain Knowledge	13
2.3.4	Further Parts of the MAC	14
3	Performance Study	17
3.1	Methodology	17
3.2	Simulation Tool	19
3.2.1	OMNeT++ Overview	19
3.2.2	SNR Generator	20
3.2.3	OFDM Simulator	21
3.3	Numerical Results	23
3.3.1	Varying the Number of Wireless Terminals	23
3.3.2	Varying the Maximum Speed within the Cell	29
3.3.3	Varying the Delay Spread	35
3.3.4	Varying the Transmission Power	40
3.3.5	Varying the Number of Used Modulation Types	46
3.3.6	Varying the Maximum Symbol Error Probability	49
4	Conclusions	52
A	Acronyms	54

Chapter 1

Introduction

Recently, theoretical studies have proven that dynamically assigning subcarriers of Orthogonal Frequency Division Multiplexing (OFDM) systems can be advantageous for the downlink of wireless cells [12] in terms of several transmission metrics, i.e. required power, achieved throughput or goodput. This result is due to the fact that subcarriers of the same Wireless Terminal (WT) experience a different channel gain caused by multipath propagation. Also the channel gain of the same subcarrier varies for different wireless terminals due to different positions of the terminals. Therefore algorithms exploiting this kind of diversity can improve the transmission of data, compared to algorithms which do not consider channel gains of various subcarriers when assigning these.

However, this system concept is based on quite strong system simplifications, which make the system improvements possible. First, it is assumed that at the access point prior to the computation of subcarrier assignments all subcarrier gains to each terminal are known. Second it is assumed that after the generation of assignments wireless terminals somehow “know” which subcarriers they have been assigned by the dynamic algorithm. In some studies the authors mention an existing out of band signaling system, but no investigation has been conducted highlighting the cost of such a signaling system.

Intuitively, the success of dynamically assigning subcarriers to terminals is directly related to the available channel knowledge at the access point: if only outdated channel knowledge is known to the access point it will not be able to assign subcarriers efficiently. In an extreme case the usage of outdated channel knowledge might even harm transmission metrics such as goodput for example. However, the access point will always have to use somehow outdated channel knowledge, the usage of the most recent channel information can not be assumed for an appropriate system study. Therefore the question arises by how much the channel information might be outdated in order to still be of usage for the system concept of dynamically assigning subcarriers.

Under the assumption that the issue of channel knowledge is not imposing to strict limitations of the system concept, the next question arising is, if the required overhead for signaling might “absorb” all the achieved gain. By statically assigning blocks of subcarriers to different terminals, signaling need is cut to a minimum (only necessary for adaptive modulation). While it is clear that an additional use of dynamic subcarrier assignments increases this system overhead, it is not clear how much this will reduce the overall systems capability to convey application information, which is of course at the end one of the most important

aspects.

The study of the two system aspects is closely related to Medium Access Control (MAC) protocol design. The reason for this is simple: a timing structure is needed, which provides a framework for signaling, receiving channel gain information from the terminals and transmitting data on the downlink. Therefore we use in this report a simple MAC protocol supporting dynamic assignments of subcarriers to wireless terminals. As dynamic assignment algorithm we choose a dynamic algorithm from [4], which assigns each terminal a certain amount of subcarriers, as determined by a subcarrier allocation algorithm. For the signaling the studied system relies on an inband signaling system, resulting in a direct impact of signaling overhead on the used system metrics. Based on this, we then study the behavior of the dynamic system and the behavior of a static comparison scheme for multiple different variations of parameters of the transmission scenario such as terminal number per cell, transmission power and delay spread.

This report is structured as the following. First we introduce the system model including the MAC structure, the signaling system and the model for the channel knowledge of the access point (Chapter 2). Then we present the results of the conducted studies. Before that we discuss our methodology and briefly give an overview of the used simulation model (Chapter 3). At last we conclude our work and highlight further areas of study (Chapter 4).

Chapter 2

System Model

2.1 Considered Scenario and Environment

We consider a cellular transmission scenario. In this, an amount of J Wireless Terminals (WTs), which are all located within a certain area, are connected to an Access Point (AP), which provides data service to the terminals (Figure 2.1). We only consider the downlink transmission in this report. Each terminal has one application running on it, which receives a constant stream of data. The data is not assumed to be delay constrained, thus this could be a file transfer for example.

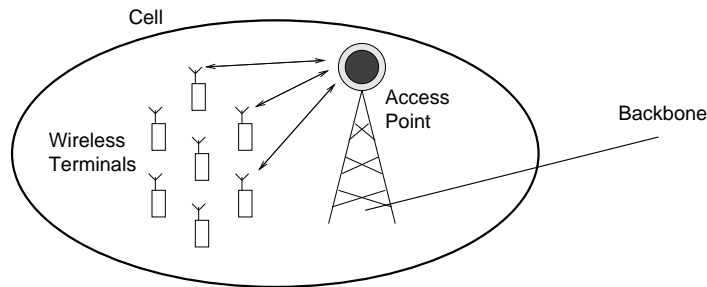


Figure 2.1: Example cellular system

The WT are allowed to roam across the area. Due to the mobility of the WTs, which is assumed to be lower than a certain maximum speed v_{\max} , the wireless channel is time variant [2]. Also the wireless channel suffers from a frequency selective behavior due to multipath propagation. The severeness of the multipath propagation is characterized by the delay spread $\Delta\sigma$. This selective behavior in time and frequency over a course much smaller than a second is also known as fading. Depending on the distance between access point and WTs is the path loss also a source of attenuation of the channel. Path loss is characterized by a reference loss occurring over some reference distance like 1 meter, this reference loss will be denoted by K . Also path loss depends on the path loss exponent, characterizing how severe a distance increase or decrease changes the attenuation of the received signal. The path loss exponent is denoted by α . Both values depend highly on the environment considered, for example is the set of K and α very different in an indoor environment than in a suburban

environment (outdoor). At last we consider the attenuation of the wireless channel to depend also on shadowing. Shadowing influences the signal strength randomly, where the probability density function of the attenuation factor is known to be log-normal distributed with a mean of 0 dB and a standard deviation depending also on the considered environment.

2.2 Physical Layer Model

As transmission scheme we assume an OFDM scheme to be employed. OFDM belongs to the class of Multi-Carrier Modulation (MCM) schemes. These schemes are characterized by splitting a given transmission bandwidth B into a set of S subbands. Data transmission is then done in parallel by the set of the different subbands, rather than serial by interpreting the available bandwidth as one monolithic wireless channel. The subbands in MCM schemes are also often called subcarriers.

The advantage of this division of the available bandwidth into S subcarriers is given by the change from serial data transmission to a parallel one. Given a high data rate source, in a Single-Carrier Modulation (SCM) scheme the data has to be transmitted serially. Therefore the transmission of a single data entity, called a digital symbol, has to be done within a short period of time. In a MCM scheme this is not required any more, since S subbands can be employed for transmission of digital symbols simultaneously. Therefore the time which may be used in order to transmit one digital symbol, called the symbol time T_s , is now increased by a factor of S . As a consequence, the transmitted symbols are not subject to an effect called Intersymbol Interference (ISI) any more, which causes severe performance degradation in systems employing SCM schemes, especially with high data rates. Throughout this report, we consider a system that employs $S = 48$ subcarriers over a total system bandwidth of $B = 16.25$ MHz, where a single symbol time requires $T_s = 4\mu s$. These values correspond to wireless local area networks following the IEEE 802.11a standard [6]. In addition we assume the subcarriers to be spaced apart by 312.5 kHz, as it is with IEEE 802.11a. The center frequency of the considered system is also picked according to the IEEE 802.11a system at $f_0 = 5.2$ GHz, which allows the usage of three different bands, mentioned in Table 2.1.

Band Name	Frequency Range
U-NII Lower Band	5.15 - 5.25 GHz
U-NII Middle Band	5.25 - 5.35 GHz
U-NII Upper Band	5.725 - 5.825 GHz

Table 2.1: Frequency Bands of the IEEE 802.11a WLAN standard

OFDM as special form of MCM schemes is characterized by a quite high spectral efficiency. The reason for this is a special frequency spacing between the different subcarriers. In traditional Frequency Division Multiplexing (FDM) a guard band is placed between each subband such that no Intercarrier Interference (ICI) occurs between the neighboring subbands. In OFDM no guard bands are employed. Instead, by placing the transmit frequencies, the so called subcarriers, by a well defined frequency difference to each other, no ICI occurs although the transmit spectra of the different subbands overlap significantly. However, at the transmit

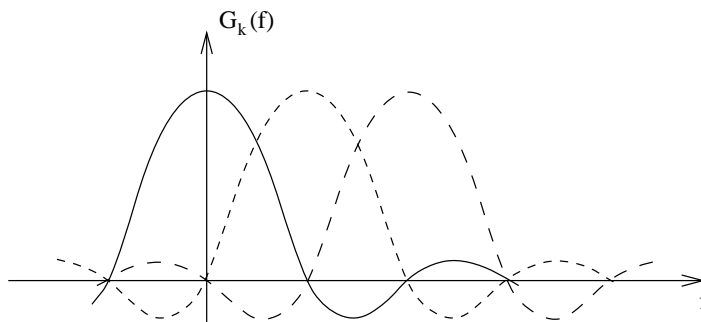


Figure 2.2: Power spectrum of different OFDM subbands. As mentioned do the transmit frequencies, the subcarriers, not interfere with each other, due to spectral nulls of all adjacent subcarriers at any given subcarrier.

frequencies of each subband, the spectral power of all other neighboring subbands is equal to zero, such that no ICI occurs (Figure 2.2). This requires the frequency spacing B_s to be related to the transmit duration of a symbol T_s by the relationship given in Equation 2.1. This special spacing causes the subcarrier frequencies to be *orthogonal* [10], hence the name OFDM. As a consequence, all subcarriers have to employ the same symbol duration T_s and therefore the same symbol rate. Here we assume that a certain bandwidth B may be utilized for transmission, which is divided into S subcarriers.

$$B_s = \frac{1}{T_s} \quad (2.1)$$

The digital data transmitted on a single subcarrier is represented by a modulation symbol. A couple of different modulation types can be used for data transmission. The modulation types differ in the amount of bits each symbol of the corresponding modulation alphabet represents. We assume here a system employing five different modulation types, which are given in Table 2.2. Most of these modulation types are also used by the wireless local area network IEEE 802.11a [6].

Modulation Type	Number of Bits represented
Binary Phase Shift Keying (BPSK)	1
Quadrature Phase Shift Keying (QPSK)	2
16 Quadrature Amplitude Modulation (16-QAM)	4
64 Quadrature Amplitude Modulation (64-QAM)	6
256 Quadrature Amplitude Modulation (256-QAM)	8

Table 2.2: Considered modulation types

Each symbol of any modulation type is transmitted with the same transmit power P_{tx} . In this report we do not assume that different transmit power levels are employed for the transmission of symbols on different subcarriers. For example is the maximum transmit power tolerated in IEEE 802.11a systems given in Table 2.3. Due to the bandwidth spacing of the

subcarriers the thermal noise power level on each subcarrier is set to $n_0 = -117$ dBm [11].

Frequency Band	Maximum Transmit Power	Power per Subcarrier
5.15 - 5.25 GHz	10 mW (10 dBm)	0.2 mW (-7 dBm)
5.25 - 5.35 GHz	50 mW (50 dBm)	1 mW (1 dBm)
5.725 - 5.825 GHz	200 mW (200 dBm)	4 mW (4 dBm)

Table 2.3: Maximum transmit power levels for different frequency bands of IEEE 802.11a

Switching from one modulation type to another is possible from one transmitted symbol to another. It is therefore not assumed, that switching requires any gap time or any other form of cost.

OFDM systems possess a high degree of flexibility. First of all it is possible to employ on different subcarriers different modulation types simultaneously. Since modulation types differ most the time in the number of bits a single symbol from the modulation alphabet might represent, this leads to the possible transmission of a different number of bits on different subcarriers per symbol. There is no downside related to this feature. An additional feature of OFDM systems is that it is possible to convey data to different receivers on different subcarriers. In any receiver in an OFDM system all data from all subcarriers is demodulated simultaneously. There is no way to receive data of certain subcarriers by not demodulating the data transmitted on the other subcarriers also. Therefore, after such a demodulation step, the receiver has to discard all data, which does not belong to him, if his data is to be conveyed on a special subset of the S subcarriers.

As described in Section 2.1 does the wireless channel constantly change due to the varying attenuation (Figure 2.3). If S subcarriers are employed in the system, then some attenuation effects will harm all subcarriers in an equal manner for each terminal, while others have a varying impact per subcarrier. Namely the fading influences each subcarrier individually, while path loss and shadowing have a similar effect to each subcarrier. In addition do both effects, shadowing and path loss influence the channel attenuation rather on a larger time scale (typically around 1 second) while fading causes changes to the channels attenuation rather on a small time scale (around 1 ms) [2]. For different WTs the subcarriers are attenuated statistically independent from each other.

Due to this behavior of the subcarriers attenuation and the offered flexibility of the considered OFDM system, it is beneficial to assign subcarriers and modulation types dynamically to different WTs. Algorithms doing this have been suggested recently [12, 15, 4] and all of them show substantial performance increases. In this report we will work with the scheme suggested as advanced Dynamic Algorithm (aDA). In short this scheme assigns subcarriers to WTs depending on their actual Channel Gain-to-Noise Ratio (CNR). After the subcarriers have been assigned, for each subcarrier a specific modulation type is chosen. We assume the transmission power to be constant on each subcarrier and then choose the modulation type with the highest representation of bits per symbol, which is able to provide a Symbol Error Probability (SEP) below a certain threshold, denoted as P_{Symbol} . Basically this is equal to assigning each modulation type a range of Signal-to-Noise Ratio (SNR) values, for which this modulation type will be used (Figure 2.4).

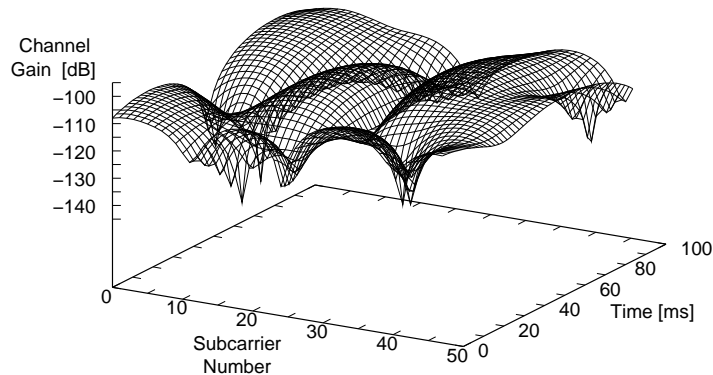
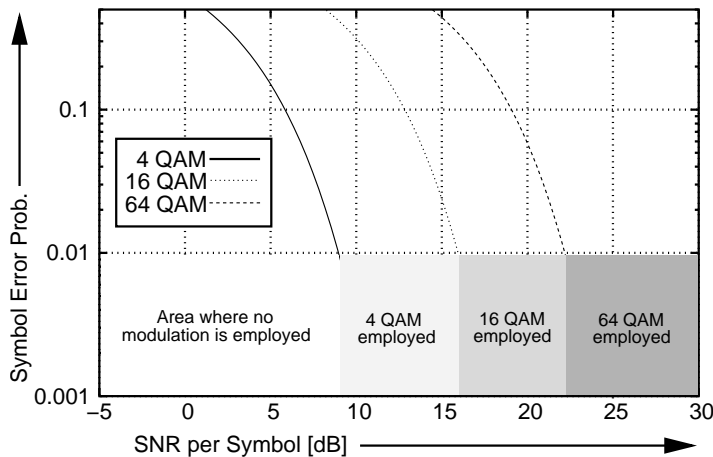


Figure 2.3: Example channel gain behavior of a frequency and time selective fading channel

Figure 2.4: Symbol error probability and example SNR modulation ranges as applied for a maximum acceptable P_{Symbol} of 0.01

2.3 Medium Access Control Layer

As mentioned in Section 2.2, depending on the actual states of the subcarriers regarding each WT, subcarriers and modulation types are assigned. However, doing this requires a couple of very fundamental conditions. First of all, before data might be conveyed via a new set of assigned subcarriers employing on each subcarrier a certain modulation type, the WTs have to be informed, which subcarriers and which modulation types they have been assigned. This is very critical information, since it determines the success of any dynamic assignment scheme. Without a signaling scheme guaranteeing exactly this precondition, a system using such a dynamic assignment scheme will not work. The second condition for a dynamic assignment scheme is that the assignments have to be rearranged every time the subcarriers change their states. However, state change is a continuous process in reality, therefore the assignments have to be rearranged every time the states have changed somewhat *significantly*. Therefore a timing structure has to be provided, which allows a regular update on the assigned subcarriers and modulation types. These two preconditions can be solved

by introducing a MAC structure, which also provides mechanisms for distinguishing between uplink and downlink phases as it usually does. We now suggest a structure which is able to guarantee the two mentioned preconditions, while it owns also other important features. In addition to this must the access point also have the information of the subcarrier states. This information can only be obtained by the wireless terminals, which transmit this information then to the access point. This shown timing structure also provides the opportunity for this.

2.3.1 MAC Timing and Frame Elements

The timing structure of the MAC layer which we will use in this study is based on a sequence of MAC frames. Every T_f one such frame is generated by the MAC layer. Throughout this report we will consider $T_f = 2\text{ms}$, which is the length of a frame in a HIPERLAN/2 system [3] (Figure 2.5). Each frame consists of a broadcast phase for the transmission of signaling information, a Downlink (DL) phase and an Uplink (UL) phase. The time durations of the three phases are denoted by T_{sig} for the signaling phase, T_d for the DL phase and T_u for the UL phase. Throughout this report we set these values such that the length of the UL phase equals the length of the DL phase plus the length of the signaling period.

For transmission of DL and UL data, two different multiplexing schemes are used, OFDM-FDM for the DL transmission and OFDM-TDMA for the UL transmission. As described in Section 2.2, during a DL phase subcarriers and modulation types are distributed dynamically, as example subcarrier assignment algorithm we choose the aDA [5].

The nature of dynamically assigning subcarriers and modulation types implies that due to subcarrier state changes different subcarriers and modulations are assigned from frame to frame. In order to inform the terminals of these changes, an additional phase is introduced. This Signaling (SIG) phase is used to send subcarrier assignment and modulation type information from the AP to all WTs in the cell. This data is transmitted as broadcast information on all S subcarriers using a fixed modulation type. Details are described in Section 2.3.2.

As mentioned we explicitly focus on DL transmissions. Therefore the UL phase is not further specified. We only assume that during this phase a Time Division Multiple Access (TDMA) scheme is used. During the UL phase the AP receives the actual SNR values of the subcarriers regarding each WT during this phase from each WT such that at the end of this phase the AP received a complete update of all subcarrier SNR values regarding each WT. Based on these SNR values, the aDA generates new subcarrier and modulation type assignments for each WT, which is sent then to each one during the following SIG phase. As mentioned above each of the three phases has its own duration. For illustration purposes we

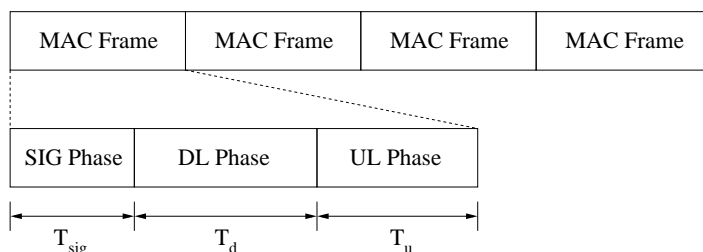


Figure 2.5: Basic MAC structure

split T_f into two equally long parts, where one part belongs to the UL phase. The other part is split into the SIG phase and the DL phase. The signaling phase is a necessary precondition for using dynamic subcarrier assignments in the DL phase, therefore the duration of each signaling phase is subtracted from the DL phase. All fixed numerical values concerning the MAC timing are summarized in Table 2.4. The calculation of the length of a SIG phase is given in Section 2.3.2.

Timing Parameter	Duration
MAC frame (T_f) [3]	2ms (500 Symbols)
Downlink phase (T_d)	0.924ms (231 Symbols)
Signaling phase (T_{sig})	0.076ms (19 Symbols)
Uplink phase (T_u)	1ms (250 Symbols)

Table 2.4: Fixed MAC timing values

2.3.2 The Signaling System

So far we have discussed the basic timing structure and the principal task of the SIG system. As outlined dynamically assigning subcarriers and modulation types to WTs is based on a reliable signaling system, otherwise a dynamic scheme can not run. In principle there are different ways to implement such a signaling system and it is not uncommon to assume an *out of band* signaling system. Such a system uses a specific communication channel for signaling the desired information to the WTs. The biggest characteristic of such a system is that it does not consume resources of the running system, since it utilizes some radio bandwidth outside of the employed transmission band. However, transmission errors or transmission latencies occurring in such a signaling system do have an impact on the provided throughput of the system. In contrast, an *inband* signaling system has a direct drawback for the provided throughput of the system, even if no transmission errors occur while conveying the signaling information. Here, the Signaling system consumes periodically for example a certain time period, during which it transmits its information via the same bandwidth other data is transmitted to or from the WTs during a different time span. In this report we choose an inband signaling system to be employed in order to study the direct trade off between throughput gained by employing a dynamic subcarrier assignment algorithm and paid throughput loss because of the need to signal these dynamic assignments first, before transmitting.

As outlined in Section 2.3.1 a certain time span is reserved for transmitting the signaling information in each frame. During this SIG phase the complete signaling information is transmitted via a broadcast transmission on all available subcarriers with a fixed modulation type (BPSK). The amount of bits and the structure used in order to transmit this information depends directly on the maximum values the scenario parameters J , S and M can take. In this report we choose these parameters to take the maximum values given in Table 2.5.

The subcarrier assignments can be interpreted as a $S \times 2$ Sub-Band Assignment Matrix (SAM), which is illustrated in Table 2.6. Each $B[J]$ stands for the size of the WT address (w) and $B[M]$ for a specific modulation type (m). Both values have to be sent to those WT

Scenario Parameter	Value
Maximum number of WT per cell (J)	64
Number of subcarriers (S)	48
Maximum number of modulation types (M)	8

Table 2.5: Maximum scenario parameter values

to which at least one of the S subcarriers is assigned. By using the operator

$$B[x] = \lceil \log_2(x) \rceil \quad (2.2)$$

and the above mentioned scenario parameter values this results in

$$l_{sam} = S \times (B[J] + B[M]) = 432 \text{ bits} \quad (2.3)$$

of information which aDA passes to the MAC system.

$B[J]_{0,0}$	$B[M]_{0,1}$
\vdots	\vdots
$B[J]_{S-1,0}$	$B[M]_{S-1,1}$

Table 2.6: Layout of the Sub-Band Assignment Matrix

In our SIG system the full SAM is included in a structure called Sub-Band Assignment Field (SAF) which is transmitted during the SIG phase to each WT in the cell. Note that the system does not transmit to each terminal separately its newly assigned subcarriers and modulation types. Instead, the complete set of assigned subcarriers and modulation types is transmitted via a broadcast. Although this procedure adds a large quantity of overhead to our system it has several benefits. All subcarriers can be used for the transmission, which results in S bits per OFDM symbol, and no WT addressing is required. Furthermore the cyclic broadcast of the full subcarrier assignment information assures a regular admission control phase for both, new members of the cell and WTs which have lost synchronization, e.g. by losing the data from the previous SIG phase.

Although BPSK is a very robust modulation scheme, bit errors might still occur. Due to the fact that one bit error during the transmission of the SAF causes the loss of the subcarrier states for at least one WT and therefore the loss of the synchronization to the AP for at least the following DL phase, i.e. until the SAF is received correctly in one of the following SIG phases, the detection and correction of transmission errors is an important issue.

Naturally this adds information to the SAF. As Frame Check Sequence (FSC) a 12 bit Cyclic Redundancy Check (CRC) [13] is used which enables the recognition of single bit errors, all errors with an odd number of inverted bits and all burst errors up to the length of the power of the used CRC polynomial $r = 12$. If all error patterns are considered equally likely, larger burst errors will be recognized with the probability of

$$P_{r,crc}(r = 12) = 1/2^{r-1} = 4.88 \times 10^{-4}|_{b=r+1} \quad (2.4)$$

for a burst length (b) of 13 and with

$$P_{r,crc}(r = 12) = 1/2^r = 2.44 \times 10^{-4} |_{b>r+1} \quad (2.5)$$

for $b > 13$ [13]. For the FSC 12 bits are added to the SAF. With the help of the FSC most of the transmission errors will be recognized but so far resynchronization is still necessary. To prevent this, a Forward Error Correction (FEC) system adds redundancy to the SAF which enables the possible correction of wrong received bits. With this in mind we use a cyclic block coding scheme, the so called BCH codes [8]. A block code can be fully specified with (n, k, d_{min}) where n stands for the length of the encoded block, k for the length of the uncoded block,

$$d_{min} \geq 2t + 1 \quad (2.6)$$

for the minimum Hamming-Distance and t for the number of correctable single bit errors. We chose a (498, 444, 13) BCH code which includes the full SAF as well as the FSC and enables the correction of $t = 6$ single bit errors (Equation 2.6) by adding $(n - k) = 54$ redundancy bits to the SAF. Assuming binomial distributed bit errors, the rest-bit-error-probability $P_{bit,CW,rest}$ [9], which includes the probability for wrong corrected as well as for non-correctable decoding errors, can be estimated by

$$P_{bit,CW,rest} \approx \frac{(2t + 1)}{n} \left(1 - \sum_{i=0}^t B(n, P_{bit}, i)\right) \quad (2.7)$$

with

$$B(n, P_{bit}, i) = \binom{n}{i} p^i (1 - p)^{(n-i)}. \quad (2.8)$$

Assuming an SEP of $P_{Symbol} = 10^{-2}$ which directly results in the Bit-Error-Rate (BER) (P_{bit})¹ (Equation 2.7) leads of

$$P_{bit,CW,rest} \approx 6.446 \times 10^{-3} \quad (2.9)$$

for the decoded SAF. With the considered scenario parameters (Table 2.5), FSC and FEC finally prolong the SAF (Figure 2.6) to 498 bits which will be sent using 10.375 OFDM symbols over all S .

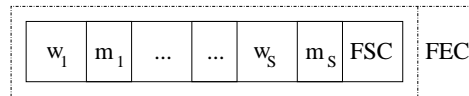


Figure 2.6: Layout of the Sub-Band Assignment Field

With the SAF the SIG phase offers a reliable broadcast of subcarrier assignment information to all members of the cell. To complete its task some additional fields (Figure 2.7) have to be added. A preamble, containing Synchronization (SYNC) field and the Start of the Frame Delimiter (SFD), enables the bit and frame synchronisation of the WT for which 8 OFDM symbols have to be reserved.

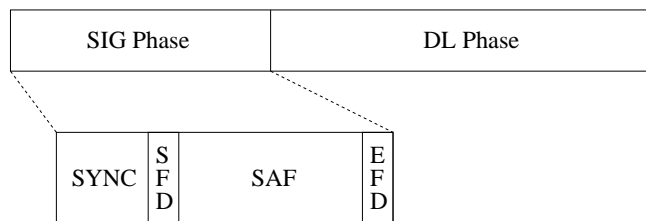
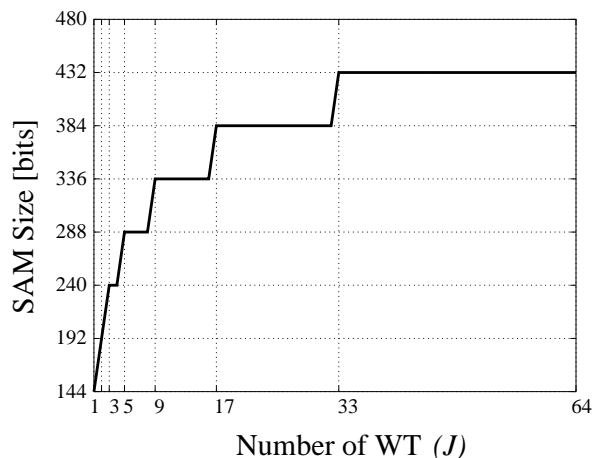


Figure 2.7: Layout of the SIG phase


 Figure 2.8: Size of the Sub-Band Assignment Matrix for $S = 48$ and $M = 8$

Since the number of WT in the cell can not assumed to be constant, the size of the SAM and therefore the length of the SAF may vary in principle (Figure 2.8). However in this technical report we consider $J \geq 64$ and therefore the size of the SAM is fixed to 432 bits.

In scenarios with a heavy variation of J , a variable SAF length is useful which implies the introduction of the 8 bit long End of the Frame Delimiter (EFD). Since the transmission of the EFD and the SAF use the same modulation scheme, both symbol times may be added. This results in $10.542 \approx 11$ OFDM symbols during the SIG phase. This finally leads to 19 OFDM symbols, including the preamble, for the transmission of the SIG phase.

2.3.3 Subcarrier Gain Knowledge

As stated above does the uplink phase provide the opportunity for the WTs to transmit their subcarrier gains to the access point. Therefore in such a system setup, the terminals would measure their channel gains during the downlink phase of MAC frame x and would transmit this information to the access point also during the uplink phase of MAC frame x . However this information would be used as subcarrier gain estimates for MAC frame $x + 1$, since based on this information the access point builds the subcarrier assignment sets. The real subcarrier gain values will differ from these estimates, the faster the subcarrier gains change (which depends directly on the maximum speed of the wireless terminals in the cell)

¹ Unless the SEP is very high, a symbol error can be assumed to result in a single bit error [10].

the more severe does a subcarrier gain change from one frame to another. Interestingly, this subcarrier state information is used as estimate for the complete MAC frame $x + 1$, or at least for the downlink phase of MAC frame $x + 1$. If subcarrier states change very fast, then even the knowledge of the subcarrier gains as they are at the beginning of MAC frame $x + 1$ are not an appropriate estimate for the whole downlink phase of MAC frame $x + 1$. Figure 2.9 illustrates the realistic subcarrier gain information at the access point.

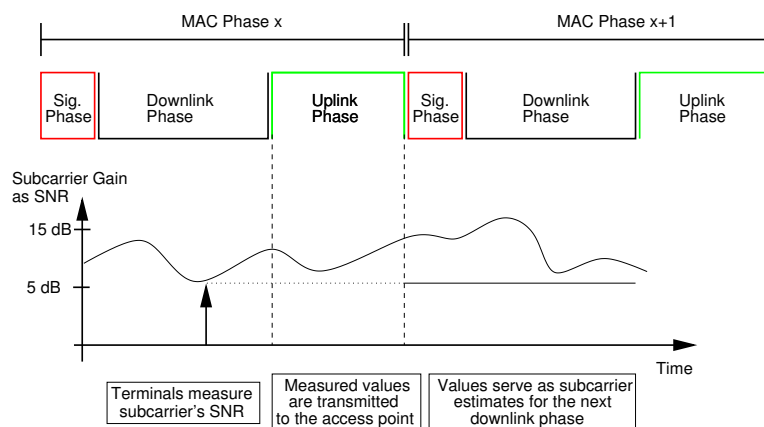


Figure 2.9: Illustration of the realistic channel knowledge at the access point for a fast varying subcarrier behavior

2.3.4 Further Parts of the MAC

This section highlights further aspects of the considered MAC layer such as frame building, frame synchronization and error control. Because these functions were already mentioned for the SIG phase, we will focus on the DL phase and briefly on the UL phase. The major task of the DL phase is to control the transmission of the so called Protocol Data Unit (PDU). In this report this term denotes a data structure delivered from the Logical Link Control (LLC) layer to our MAC system. It contains control information of the upper layers and finally the payload.

On the MAC layer the PDU is included in a subframe, which contains several additional fields (Figure 2.10). Since at the end of the SIG phase the transmission scheme changes from a BPSK modulated broadcast on all S subcarrier to one of the M modulation types transmitted on N subcarriers, the DL phase needs its own preamble to assure bit and frame synchronization. Thus it starts with the SYNC field which contains 64 alternating bits which is followed by the SFD, containing the characteristic sequence 01111110. Bit-stuffing assures that this sequence will not appear in other parts of the frame. The SFD is followed by the PDU and the FSC which contains a CRC of the PDU. Both fields are encoded using BCH codes. Due to the variable m , which results in different numbers of bits (Table 2.2) modulated on a single symbol (m_t), the bit size of the PDU may vary from frame to frame. Considering 231 OFDM symbols which are transmitted using N subcarriers and m_t bits/symbol (regarding the modulation type chosen by aDA) the length of the PDU (l_{pdu}), including $(n - k)$ redundancy

bits added by the FEC and l_{fsc} bits for the FSC, can be expressed by

$$l_{pdu} + (n - k) + l_{fsc} = N \times (m_t \times 231). \quad (2.10)$$

Since all the above mentioned parameters are known by the WT the usage of an EFD is unnecessary. Table 2.7 lists the bit sizes of all DL phase fields and illustrates the variation in size of the error coded PDU for the considered modulation types.

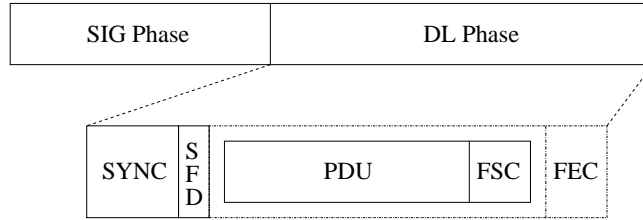


Figure 2.10: Layout of the DL phase

Field	m_t [bits/symbol]	Length [bits]
Synchronization field	independent	64
Start of the Frame Delimiter	independent	8
PDU including l_{fsc} and $(n - k)$ redundancy bits	1	477
	2	1386
	4	2772
	6	4158

Table 2.7: DL phase fields

The properties of the CRC code used for the FSC are similar to those of the above mentioned CRC-12. We use a CRC-24 polynomial ($r = 24$) which results in a CRC of $l_{fsc} = 24$ bits and enables the recognition of single bit errors, all errors with an odd number of inverted bits and all burst errors up to the length of r . If all error patterns are considered equally likely larger burst errors will be recognized with the probability of $P_{r,crc}(r = 24) = 1.192 \times 10^{-7}|_{b=r+1}$ (Equation 2.4) or $P_{r,crc}(r = 24) = 5.960 \times 10^{-8}|_{b=r+1}$ (Equation 2.5). Since l_{pdu} is considered to be variable in terms of the chosen modulation type different BCH codes have to be used for the FEC. All the codes achieve $t = 8$. Since the maximum length of the uncoded block (k), which depends on the chosen code, may not exceed 943 bits [8], the uncoded PDU and SAF have to be split up into

$$j = \frac{l_{pdu} + l_{fsc}}{k} \quad (2.11)$$

parts, each of length k , if its length ($l_{pdu} + l_{fsc}$) exceeds this value. If j is not an integer the PDU is filled up using zero padding which causes additional overhead. If k is greater than the size of the uncoded PDU the code is shortened and no segmentation is done ($j := 1$). With Equation 2.11 the length of the uncoded PDU can be expressed by

$$l_{pdu} = (j \times k) - l_{fsc}. \quad (2.12)$$

The resulting BCH-codes as well as the values for j are given in Table 2.8.

m_t [bits/symbol]	BCH-code [$j \times (n, k, d_{min})$]
1	$1 \times (477, 405, 17)$
2	$2 \times (693, 613, 17)$
4	$3 \times (924, 844, 17)$
6	$5 \times (831, 751, 17)$ (5 bits are padded with zeros)

Table 2.8: DL phase FEC parameters

Chapter 3

Performance Study

3.1 Methodology

As mentioned, the aim of this study is to highlight first of all the benefit of dynamically assigning subcarriers to WTs under more realistic conditions than studied before. We intend to investigate the impact of an implemented signaling system and realistic channel knowledge to the performance behavior of the dynamic algorithm. As basic comparison scheme we choose a static scheme where each WT receives a fixed set of subcarriers throughout the considered simulation time. This static scheme still employs adaptive modulation. Note that this static FDMA systems with adaptive modulation behaves equal in terms of the considered metrics to a TDMA system with adaptive modulation.

As metric we consider two in the further study: average throughput per WT in bits per second and average packet goodput per WT in packets per second.

For the study we vary certain parameters in order to investigate the behavior of both static and dynamic schemes for different *environments*. We define a basic setting and vary one parameter at a time from this basic setting which is studying the system in multiple, related environments. The basic setting is given in Table 3.1.

Out of these six parameters we choose one at a time and vary this parameter then. The resulting variations per parameter are given in Table 3.2.

The results are obtained via simulation. For each parameter setting, hence for each

Parameter	Setting
Number of Wireless Terminals	16
Transmission Power	-7 dBm
Maximum speed of the terminals	$1 \frac{\text{m}}{\text{s}}$
Delay Spread	150 ns
Used Modulation Types	BPSK, QPSK, 16-QAM, 64-QAM, 256-QAM
Maximum Symbol Error Probability	10^{-2}

Table 3.1: Basic parameter setting for the study of dynamic and static subcarrier assignment schemes

Parameter	Variation Points
Number of Wireless Terminals	From 1 to 48
Transmission Power	From -16 dBm to 3 dBm
Maximum speed of the terminals	From $1 \frac{\text{m}}{\text{s}}$ to $50 \frac{\text{m}}{\text{s}}$
Delay Spread	From 50 ns to 300 ns
Used Modulation Types	BPSK, QPSK, 16-QAM, 64-QAM, 256-QAM BPSK, QPSK, 16-QAM, 64-QAM BPSK, QPSK, 16-QAM BPSK, QPSK BPSK
Maximum Symbol Error Probability	From 10^{-1} to 10^{-3}

Table 3.2: Variation points for each parameter

environment, we obtain the average absolute throughput and goodput values per WT for the dynamic algorithm and the static scheme considering three different *scenarios*.

The first scenario corresponds to an ideal one, which means that signaling the assignment information causes no cost as well as perfect subcarrier knowledge can be assumed. Perfect subcarrier knowledge refers to the case where the access point has, prior to MAC frame x , the subcarrier state information of each subcarrier regarding each WT as they are at the beginning of this just starting MAC frame x . Subcarrier gains might still change during MAC frame x , but it is the most ideal case that can be assumed and corresponds to what is usually assumed if dynamic subcarrier algorithms are studied.

The second scenario is a semi-realistic case where still perfect subcarrier gain information is assumed, but the introduced signaling system is now active, thus causing a certain cost for the dynamic and static scheme (refer to Section 2.3.2). For the static scheme, still the used modulation types have to be signaled which consumes some resources, while in the case of the dynamic algorithm subcarrier assignments as well as used modulation types are signaled which costs more resources (Equation 2.3). If an error occurs within the signaling portion the following data transmission is discarded completely.

The third scenario, called realistic scenario, considers realistic subcarrier gain information to be present at the access point, as explained in Section 2.3.3 as well as an active signaling system for both the static and dynamic algorithm.

After obtaining the average throughput and goodput values for the two different algorithms considering the three different scenarios for each parameter setting (producing 12 different values per setting), we build ratios in order to compare the dynamic algorithms performance with the one of the static scheme. Two different ratios are used in this study for each throughput and goodput. The first ratio compares the absolute throughput or goodput values of the two algorithms **within each scenario**. For example here the absolute throughput of the dynamic algorithm in the ideal scenario is compared to the absolute throughput of the static scheme in the ideal scenario, the throughput of the dynamic in the *realistic scenario* is compared to the static in the *realistic scenario*. This Scenario-Bounded Ratio (SBR) reveals the performance gain or loss of the dynamic algorithm compared to the

static algorithm considering the effort to be taken into account for **both** cases. Here no cross comparison between the performance of the different dynamic results for the three scenarios can be deduced.

The second ratio, called Inter-Scenario Ratio (ISR), compares the absolute value, either throughput or goodput, of the dynamic algorithm for each scenario with the absolute value achieved by the static scheme in the **ideal scenario**. Therefore for the previous example the other ratio is built by comparing the throughput of the dynamic algorithm in the *realistic scenario* with the throughput of the static scheme in the *ideal scenario*. Here information can be obtained about the different performance behavior of the dynamic algorithms for the three scenarios compared to each other. Also in this ratio the dynamic results of the realistic case are compared to the static results using the most optimistic system assumptions possible. If the dynamic stills outperforms the static, this is a clear statement for using a dynamic algorithm instead of a static Frequency Division Multiple Access (FDMA) or static TDMA system set up.

3.2 Simulation Tool

The simulation process comprises two components, the generation of the channel gains (SNR Generator) and the actual OFDM system (OFDM Simulator). It is divided as such to accommodate the reuse of the data, which would otherwise be tediously and redundantly calculated throughout the simulation and also to speed up the whole process. The simulator, including the design and implementation, are outlined in the following sections, but first, a very general introduction into the simulation tool, OMNeT++, is given.

3.2.1 OMNeT++ Overview

OMNeT++ is an object-oriented discrete event simulation tool which allows the modeling of communication protocols, computer networks, traffic models and basically any other system that may use a discrete event approach. It consists of a hierarchy of so-called modules, both simple and compound, whose behavior and functionality is user-defined. These simple modules are the fundamental building blocks of the simulator and are clearly the lowest entity in the hierarchy. A system may easily be constructed using merely these units, however they are more commonly combined together into compound modules to more realistically model the structure of data communication systems and networks.

These modules are interconnected through a series of gates and channels and they communicate with each other via messaging. The messages are defined by the simple modules and they can contain arbitrarily complex data structures. The connections are simple ideal paths that allow the transfer of these messages, however, they may also be complex routes, such that error rates, data rates and propagation delays may be specified to obtain certain desirable channel characteristics.

OMNeT++ also offers a wide range of additional functionality, including routing support and statistical analysis, and therefore, for greater insights into the simulation tool, the manual should be consulted [14].

3.2.2 SNR Generator

The SNR Generator models a Wireless Terminal roaming through a square cell and consists of both the terminals and the AP, as shown in Figure 3.1. A destination point is randomly generated within the cell and the terminal moves immediately to this point, traveling always in a series of straight lines and with a maximum speed of v_{max} (Table 3.2). Once this goal has been reached, a new point is again calculated and the terminal continues in the same manner.

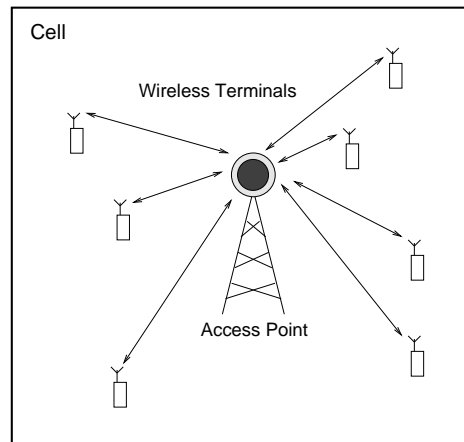


Figure 3.1: SNR Generator – Movement of a Wireless Terminal

As the WT traverses the cell, the subcarriers or wireless channels undergo different time-varying effects, which are described in Section 2.1. The first of these effects, path loss, arises simply due to the distance between the AP and the WT. It is characterized by two constants, the path loss exponent (α) and a reference loss (K), and is modeled in the simulation using a standard equation.

Shadowing is a random signal attenuation or gain resulting from obstacles, such as buildings, cars, or mountains, obstructing the path of a signal. It is modeled using a normal, Gaussian distributed probability density function with a mean and standard deviation dependent on the considered environment.

The last of these effects is fading; a frequency-selective, time-varying signal degradation caused by the multi-path nature of signal propagation. When a signal is transmitted, there are numerous possible paths of that it may take. As a result, multiple copies of the original signal are received at different delayed times. The severity of this is strongly dependent on the terminal speed, as well as the delay spread of the received signals.

Because of the characteristics of these attenuations, the frequency of these calculations, which is dependent on the v_{max} of the WT, varies. For example, for a WT moving at 1 m/s, the path loss and shadowing are calculated once per second and fading is calculated every DL phase. However, if this speed is increased, these values are computed v_{max} times more frequently. That means, for a WT with v_{max} equal to 50 m/s, the path loss and shadowing are calculated 50 times per second and the fading, 50 times per DL phase.

This computation frequency requires a significant amount of time and would, as a result, slow down the whole process, were the SNR Generator and the OFDM Simulator combined

together. The devised intermediate step between the simulator and generator is therefore the creation of a so-called SNR trace file. During the simulation run, the generated SNR values (fading loss, shadowing, path loss) are summed together and outputted to the file for the later use as the input to the OFDM Simulator. As mentioned above, this intermediate procedure of creating the SNR trace file allows the reuse of data and avoids the redundancy of continually recalculating these values.

3.2.3 OFDM Simulator

The OFDM Simulator models the DL phase of an OFDM-based system with inband signaling and is comprised of both the WT and AP as shown in Figure 3.2. Quite generally, the Base Station interprets the channel states into Modulation Types and performs the necessary calculations to assign all subcarriers to the different terminals in the cell. This assignment information is then made known to the WTs and the MAC statistics, such as goodput, raw throughput and error rates, are determined.

Consequently, since the report only elaborates on the signaling and the structure of the DL phase, the UL phase is no more than an empty time slot that has been accounted for in the simulation, but it performs no relevant tasks.

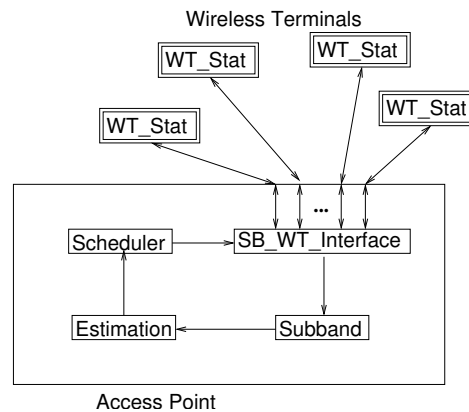


Figure 3.2: OFDM Simulator Modular Structure

SB_WT_Interface Module

As the name suggests, this *SB_WT_Interface* is the wireless interface between all WTs and the AP. Not only does it provide this communication medium between the two units, but it always plays an important role in the general timing structure of the system.

For the MAC frame, it is assumed that the channel states are valid for the time length, T_c . This means, that though the channel is continually changing, the effects are essentially negligible for a state-change time of T_c seconds. Also, regardless of the dynamic channels, the Sub-Band (SB)-WT assignments are assumed valid for some reassignment time, T_r seconds. *SB_WT_Interface* indicates to the other modules of the AP when it is necessary to recalculate the channel states and also when it is necessary to generate new subcarrier assignments.

The initiation and termination of the simulation is also controlled by this module. Once all WTs have completed their transmission, *SB_WT_Interface* is informed of this event, a final set of statistics is out putted immediately before the simulation terminates.

Subband Module

The Subband Unit's role is to interpret the states of the different channels and map these values into their corresponding Modulation Types (i.e. BPSK, QPSK). The Module reads in the externally generated SNR trace files into a structure known as a SNR Matrix (SNM), which is a $S \times J$ matrix containing the channel gains for the S subcarriers and the J Wireless Terminals in the cell. The individual SNR values are then extracted and mapped into the different Modulation Types shown in Table 2.2 and placed in a form known as a Sub-band State Matrix (SSM). The SSM is once again a $S \times J$ matrix, such that the row-column intersections represent the Modulation Type of the particular wireless terminal and subcarrier.

Both SSM and SNM are identical in structure, which is shown Table 3.3 below, and both contain the channel state information $X_{s,j}$, but in two different forms: the SSM represents the channel in terms of Modulation Types and SNM represents the channel in terms of SNR gains.

$X_{0,0}$	$X_{0,1}$	\dots	$X_{0,J-1}$
$X_{1,0}$	$X_{1,1}$	\dots	$X_{1,J-1}$
\vdots	\vdots	\dots	\vdots
$X_{S-1,0}$	$X_{S-1,1}$	\dots	$X_{S-1,J-1}$

Table 3.3: Structure of the Sub-band State and the SNR Matrix

Scheduler Module

The Scheduler Module's task is to "schedule" the resources in the system. Once the SSM has been created, the subcarriers can readily be assigned to the WTs. The SSM is examined and depending on the selected assignment algorithm described in [5], the subcarriers are assigned accordingly. This process creates a $S \times 2$ SAM (Section 2.3.2) containing the information about all subcarriers, their assigned WT and the corresponding Modulation Type, which is later transmitted during the Broadcast SIG Phase of the MAC frame.

WT_Stat Module

After the subcarrier assignment is made, the *SB_WT_Interface* begins transmitting the MAC frames to the WT. *WT_Stat*, which is a module within the WT, receives some information describing its assigned subcarriers, their modulation types and the number of errors that have arisen. Following the structure of the MAC frame in Figure 2.7 and Figure 2.10, the different components (Signaling, PDU) are extracted and the various statistics, such as raw throughput, goodput and error rates are computed and out putted to statistical files.

3.3 Numerical Results

In this study we varied various different scenario parameters, which are related to the transmission of data as well as to the transmission environment. The varied parameters are only a subset of parameters, which could be varied, though they represent the most likely ones to be changed. Considering the standard transmission scenario described in Table 3.1, we varied each time only one parameter. The results of these studies are discussed below.

3.3.1 Varying the Number of Wireless Terminals

At first let us consider a variable number of Wireless Terminals in the cell. We chose the following numbers of Wireless Terminals in the cell as environments: 1, 2, 3, 4, 6, 8, 12, 16, 24, 48. Obviously, since we have a fixed bandwidth for data transmission, a higher number of Wireless Terminals leads to lower throughput and goodput rates per Wireless Terminal since each Wireless Terminal will receive less and less subcarriers per frame. On the other hand increasing the number of Wireless Terminals in the cell increases the number of states per subcarrier. The subcarrier state diversity in the system increases (note that for different Wireless Terminals the subcarrier state behavior is statistically independent). This increase in diversity leads to a better utilization of subcarriers for adaptive schemes in the system.

In Figures 3.3 and 3.4 the absolute values for the throughput and goodput results are shown always for all three scenarios for the dynamic and static scheme. We find that in general the absolute values decrease with an increasing number of Wireless Terminals. The quantitative and qualitative behavior for throughput and goodput are same considering the dynamic algorithm as well as the static scheme.

In order to discuss the behavior of the different scenarios consider the ratios shown in the Figures 3.5, and 3.6. In general the qualitative behavior of the ratios is the same: they all increase while the number of Wireless Terminals increases within the cell. For the throughput there is no difference between the semi-realistic scenario and the realistic scenario which is quite clear since considering slightly outdated subcarrier state information does not change the statistics of the subcarrier states themselves, therefore the throughput does not change for the real scenario compared to the semi-realistic scenario. Compared to the ideal scenario the two other scenarios loose a ratio value of 0.03 due to signaling which is exactly what should be expected. Interestingly for the throughput ratios a value of 1.5 seems to be an upper bound. Even for a higher number of terminals in the system no higher ratio is found, the ratio curves are flat beginning at 16 Wireless Terminals in the cell.

For the goodput this qualitative behavior changes slightly. First of all for almost all curves there is a steady increase up to 48 Wireless Terminals in the cell. Considering the Scenario-Bounded Ratio for the goodput clearly the advantage of the dynamic scheme can be seen. While for the ideal and semi-realistic scenario the ratios increase up to 1.6 (where the ideal ratio is slightly higher due to no signaling overhead), the ratio for the realistic scenario increases up to 1.9. Note that the absolute goodput achieved by the dynamic algorithm is lower for the realistic scenario compared to the two other ones (as seen in the Inter-Scenario Ratio). But in relation to the corresponding static goodput for each scenario the dynamic algorithm gains stronger in the realistic scenario than in the other two scenarios. Therefore not utilizing dynamic subcarrier scheduling but only adaptive modulation in a

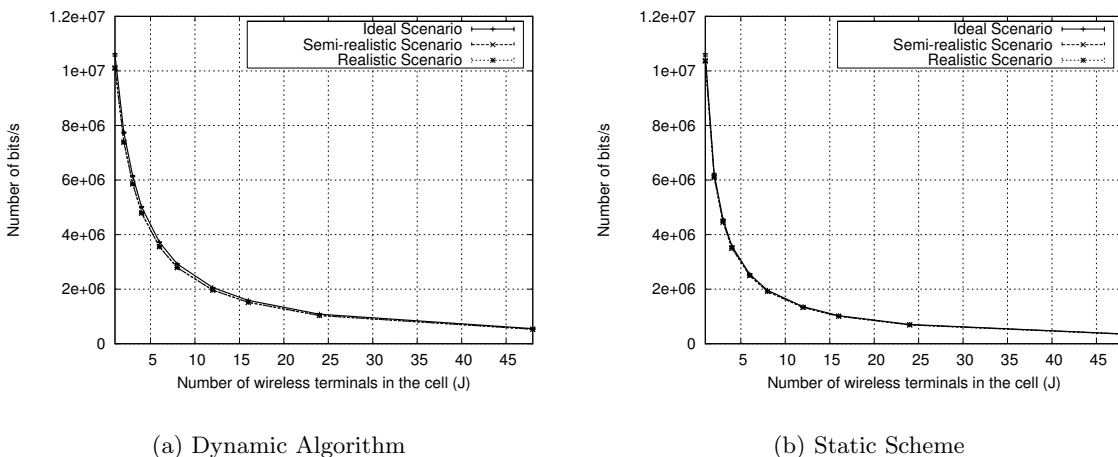


Figure 3.3: Logarithmic plots of absolute throughput of the dynamic and the static scheme for all scenarios with an increasing number of Wireless Terminals in the cell

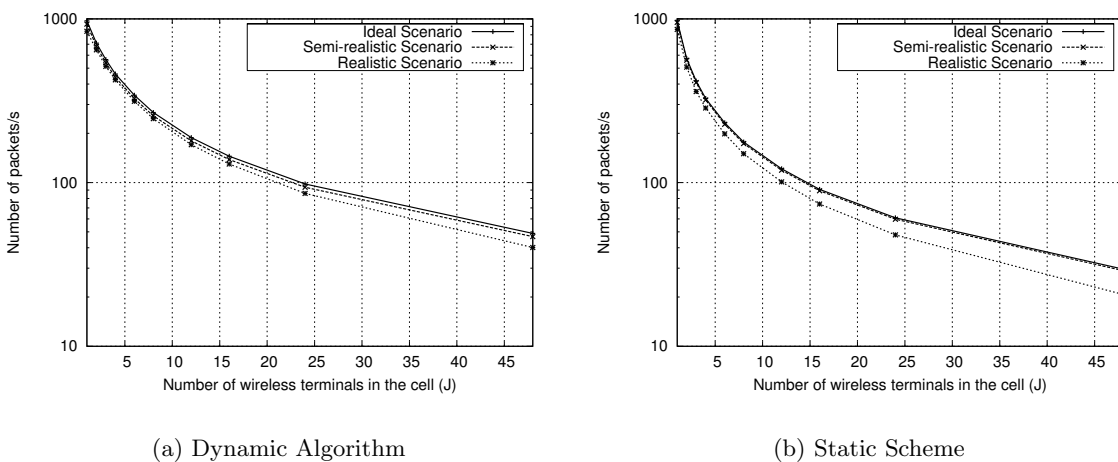
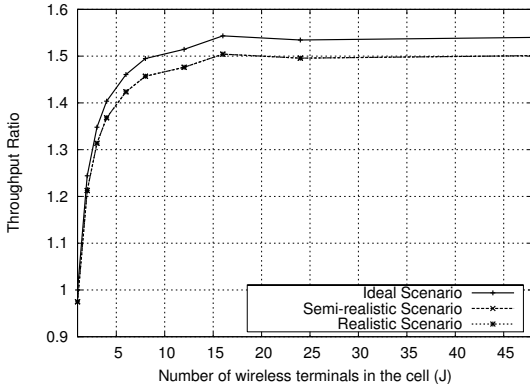


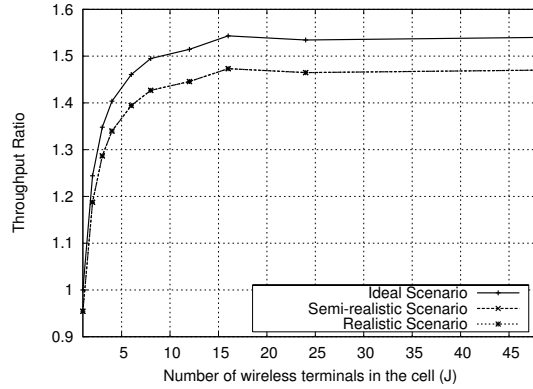
Figure 3.4: Logarithmic plots of absolute goodput of the dynamic and the static scheme for all scenarios with an increasing number of Wireless Terminals in the cell

realistic environment achieves a goodput of almost only half the goodput that might be achieved by a similar dynamic algorithm, although this is not the case for the throughput.

The throughput gain found for the dynamic scheme can be investigated further by considering the probability of assigning each specific modulation type during a downlink phase. These so-called *assignment probabilities* for the dynamic and the static scheme found in the realistic scenario are illustrated in Figure 3.7. The comparison highlights clearly the origin of the overall performance gain of the dynamic scheme compared to the static one. As the number of wireless terminals in the cell increases, the probability of assigning a higher modulation type (better than BPSK) rises. While the highest two modulation types 256- and 64-QAM may be chosen with a probability of 73% with dynamic scheduling, for example for

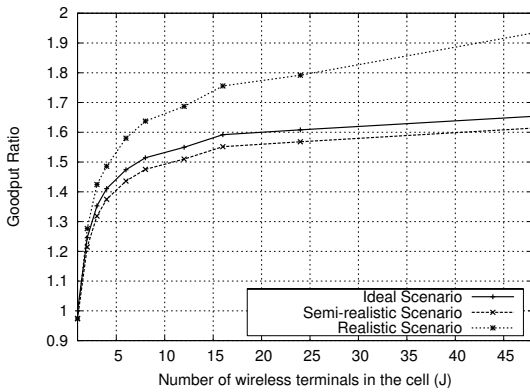


(a) Scenario-Bounded Ratio

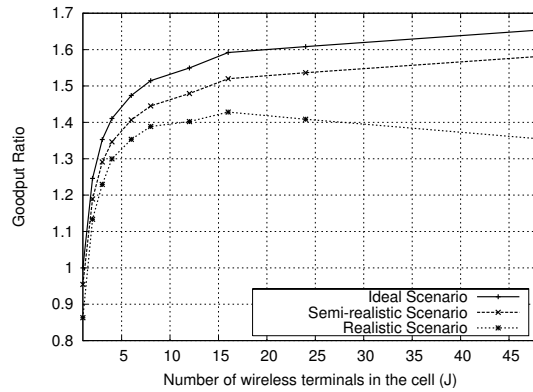


(b) Inter-Scenario Ratio

Figure 3.5: Throughput ratios for all scenarios with an increasing number of Wireless Terminals in the cell



(a) Scenario-Bounded Ratio



(b) Inter-Scenario Ratio

Figure 3.6: Goodput ratios for all scenarios with an increasing number of Wireless Terminals in the cell

48 WTs in the cell, with the static scheme this is only likely to be in 42% of the cases.

Interestingly, for *both* schemes the assignment probabilities increase with an increasing number of terminals in the cell (for the higher modulation types). However, in the case of the static scheme this increase is due to the fact that the more terminals are located in the cell the more terminals will also be quite close to the access point due to the assumed uniform terminal density in the cell. In the case of the dynamic scheme the increase of assignment probabilities for higher modulation types is stronger than in the case of the static scheme. This additional increase is due to multi-user diversity.

The ratio of the assignment probabilities of the two algorithms (results for the dynamic scheme divided by those for the static scheme) is presented in Figure 3.8. For the QAM

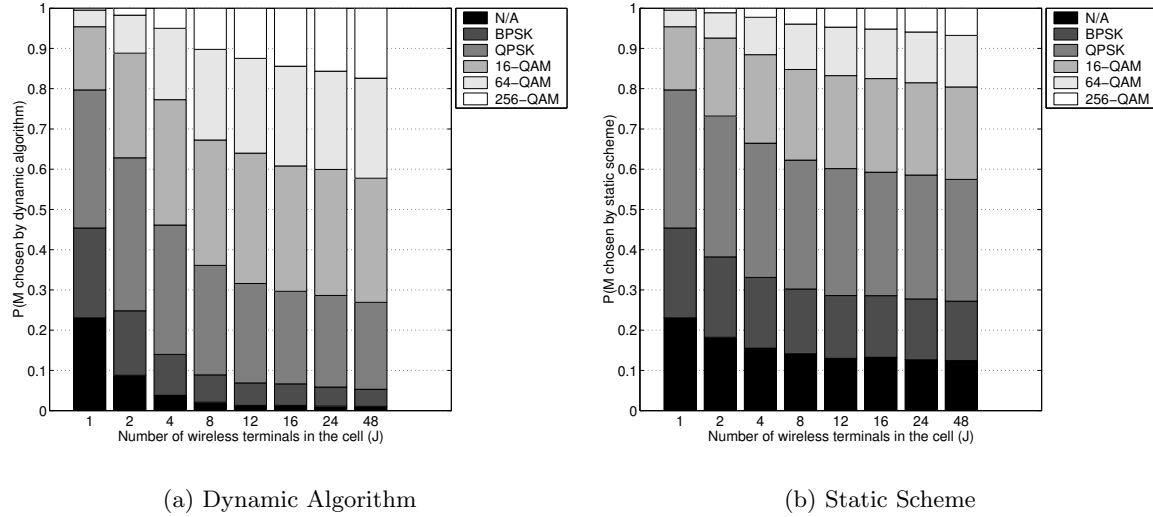


Figure 3.7: Probabilities for the assignment of a specific modulation type for the dynamic and the static scheme in the realistic scenario vs. an increasing number of Wireless Terminals in the cell

modulation types a steep increase is shown versus rising WTs in the cell until the maximum is reached for all three QAM types at 16 WTs. Here the value found for the 256-QAM ratio of 2.78, means for example that the probability of scheduling 256-QAM is 178% higher with the dynamic assignment algorithm than with the static scheme. While the probabilities for the QAM types chosen by the dynamic algorithm are rising, they decrease for the lower modulation types and for no possible assignment (N/A). While only at 4 WTs in the cell QPSK is likely to be scheduled more often with the dynamic scheme all other results for the QPSK, BPSK and N/A ratio are smaller than one, which means that those modulation types are more likely with the static scheme. If the number of WT exceeds 16 the slope of all modulation types basically stays constant, which indicates that the throughput gain does not significantly increase after this point.

However, this is not the case for the goodput. Here still an increase for $J > 16$ can be found for the scenario-bounded ratio. This can be explained by investigating the so-called *overestimation error* of the dynamic and the static assignment schemes. An overestimation error occurs if for a specific downlink phase a higher modulation type is chosen due to realistic channel knowledge than performed with perfect channel knowledge – therefore the channel is overestimated. This will result in a higher BER which affects the goodput-rate, i.e. the number of correctly received packets per second, if the bit-errors can not be corrected by FEC (designed for symbol error rates lower than the threshold). Note that channel overestimation may also occur always if the channel knowledge is not perfect. In the following we will investigate the overestimation error for the realistic scenario, where imperfect channel knowledge is assumed.

Characterizing the overestimation error decomposes into two parts: How often is an assignment performed while overestimating a channel (calling for the overestimation probability

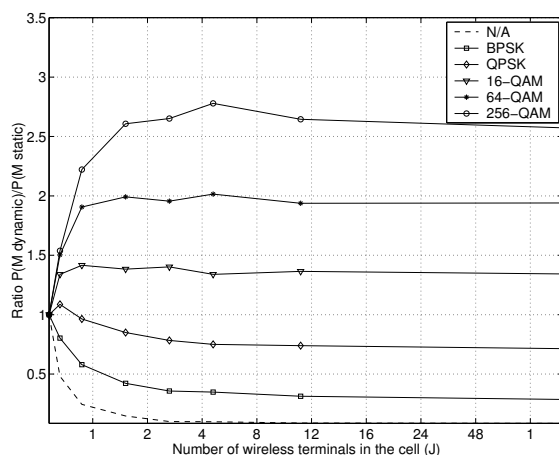


Figure 3.8: Comparison of the assignment probabilities of the dynamic vs. the static scheme in the realistic scenario for an increasing number of Wireless Terminals

per modulation type per assignment scheme) and by how much is a channel assignment overestimated on average (calling for the average overestimation error in dB).

In Figure 3.9 the overestimation probability is shown for the dynamic and the static scheme separately for the five considered modulation types. Common is for both assignment schemes that the likelihood of an overestimation error decreases with rising amounts of WTs in the cell until the minimum is reached at 16 WTs. Then the slope slightly increases for setups with higher numbers of WTs. In general higher values are found for higher modulation types, e.g. with 256-QAM the probability of channel overestimation is about 50% for one WT. While for a single WT in the cell the results for both assignment schemes are equal, the decrease of the error probability starts earlier in the dynamic case, which explains the high goodput gain for the low numbers of WTs shown in Figure 3.6. Although the minimum value at 16 WTs is smaller with the static scheme, the increase for setups with more WTs lasts to higher values than the dynamic scheduling.

In addition to the likelihood of an overestimated channel assignment, the impact of the overestimation error can be investigated by the mean of the overestimation error as shown in Figure 3.10. Here the mean difference of the SNR boundaries between the correctly and erroneous selected modulation type is illustrated separately for each modulation type. The higher this difference is, the higher the incorrectly chosen modulation type and the resulting SEP increase. As with the probability of an overestimated assignment, the mean overestimation error decreases for both assignment schemes for an rising amount of WTs in the cell until the minimum is reached at 16 WTs. The higher decrease and the very slight increase, compared to the static scheme, for scenarios with more than 16 WTs indicate another source of the benefit for the goodput if the dynamic algorithm is employed. Although the mean of the overestimation error decreases for the higher modulation types for the static scheme, this is not beneficial, since the probability of the choice of these modulation types is much smaller than with the dynamic algorithm (Figure 3.7). Note that in absolute figures the overestimation error is higher for the static scheme than for the dynamic scheme.

From the graphs of the average overestimation error the reason for the goodput ratio

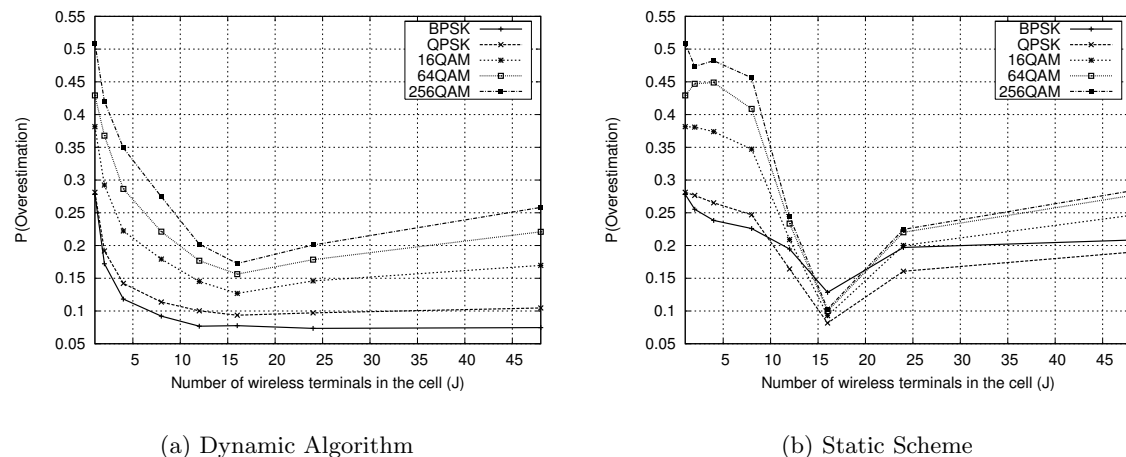


Figure 3.9: Probabilities for the overestimation of the channel state for the dynamic and the static scheme in the realistic scenario vs. an increasing number of Wireless Terminals

increase beyond the point of $J = 16$ terminals in the cell can be seen (Figure 3.6(a)). Up to 16 terminals in the cell the average overestimation error decreases for all modulation types in case of the dynamic scheme. Beyond this point a small increase can be observed. For the static scheme the overestimation errors increase instead initially before they decrease for all modulation types (starting at 12 terminals in the cell). At 16 terminals in the cell the overestimation error is minimal, beyond that point a sharp increase can be observed for the static scheme. As this sharp increase harms the packet error rate a lot for the static case, the goodput ratio increases.

We can summarize the results as the following. For an increasing number of Wireless Terminals it becomes more and more beneficial both in terms of throughput and goodput to utilize dynamic algorithms compared to a static subcarrier assignment. Signaling is not a factor that limits the system too much, however working on realistic channel information, thus outdated information, reduces the goodput of the system. This occurs much more for the static scheme the higher the number of terminals is in the cell than it does for the dynamic algorithm.

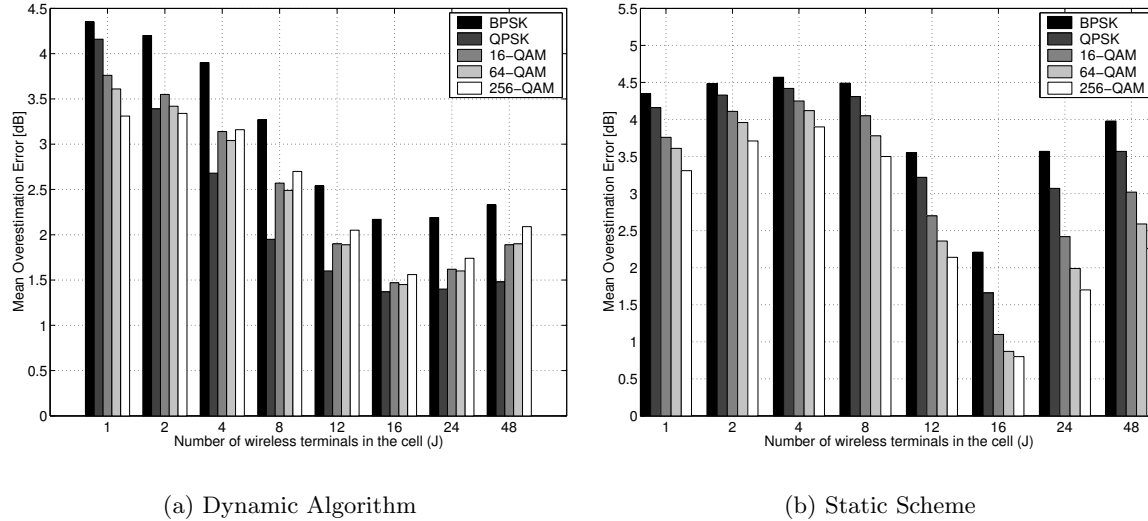


Figure 3.10: Mean values of the overestimation error for the dynamic and the static scheme in the realistic scenario vs. an increasing number of Wireless Terminals

3.3.2 Varying the Maximum Speed within the Cell

Next we varied the maximum speed of the terminals within the cell. Increasing the speed of the terminals leads to a faster fading of the subcarriers. A good measure for the “rate” of the fading is the coherence time, defined in [10]. We chose the following maximum speed values: 1, 2, 5, 10, 25, 50 ms. These values correspond to coherence times of 12.5, 6.25, 2.5, 1.25, 0.5, 0.25 ms for the considered transmission frequency band of 5.2 GHz [1]. The length of a frame was kept fixed at 2 ms.

In Figures 3.11 and 3.12 the absolute values for the throughput and goodput of the dynamic and static scheme are shown for the three different scenarios. For the absolute throughput over the course of the different considered speeds no significant change of the values can be found, only slight variances occur. Up to the speed of 25 m/s the absolute throughput increases slightly and decreases after that. However, considering the shown confidence intervals (99% confidence level), there is basically no significant increase at all although the subcarrier states change now faster and faster and by this the diversity in the system is increased over time. For the different scenarios the ideal is again slightly better than the semi-realistic and realistic, which are both equal in terms of throughput. This is the case for the static scheme also.

For the absolute goodput values however, this behavior completely changes. For both, the dynamic algorithm as well as the static scheme average goodput rates drop dramatically for an increasing speed of the Wireless Terminals. For the dynamic algorithm the drop starts at a speed of 2 m/s, after a slight increase, for the static scheme the drop starts right away from 1 m/s. Also there is a huge difference between the single scenarios. This is better observed with the throughput ratios, which are given in Figure 3.13. Since the absolute throughput values behave more or less constant, the ratios have the same behavior for the throughput.

Only slight variations can be observed around a constant ratio of 1.5. Again, due to signaling, the ratio loss for the semi-realistic and realistic scenario is around 0.03 compared to the ideal scenario.

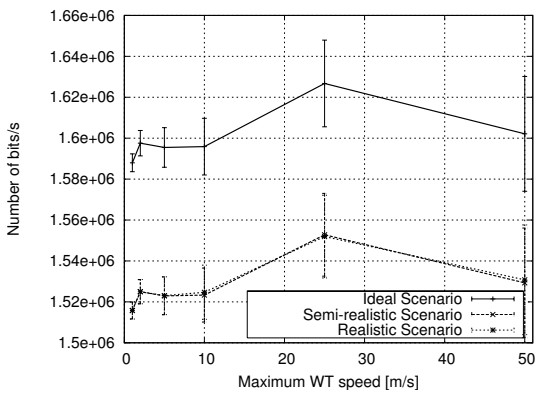
The ratios for the goodput are shown in Figure 3.14. Here a complete different situation is shown compared to the case of the absolute goodput values. While for the ideal and semi-realistic case the ratios initially increase up to a speed of 5 m/s and are also quite high for a speed of 10 m/s, the realistic case drops very drastically down to ratios below 1 already for a speed of 10 m/s. Such low ratios occur to the ideal and semi-realistic case, too, however they are reached not until the speed equals at least 20 m/s. For a varying speed this reveals the advantage of having up-to-date subcarrier state information. Especially for a higher speed this becomes crucial for the performance of the system (not in terms of throughput, only in terms of goodput!). The accuracy of the subcarrier state information is mainly determined by the length of the frame. Therefore an adaption of the frame length for faster terminal speeds is the most important message from the study of the varying speed.

To analyze this behavior of the goodput, two aspects of the scheduling system are further analyzed: First the probabilities for the assignment of a specific modulation type, secondly the nature, i.e. value and probability of occurrence, of the overestimation error.

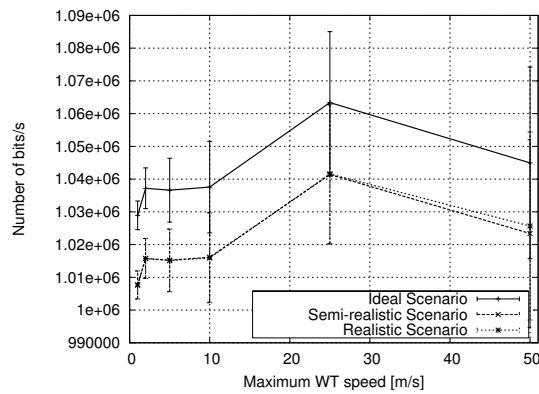
The probabilities for the assignment of a modulation type are shown in Figure 3.15. In general no significant change shows up for the rising WT speed, which basically reflects the behavior of the throughput ratios. This is reasonable since the primary channel statistics are not changed by a higher or lower velocity, only the secondary statistics.

Unlike the probabilities for the assignment of a modulation type, the likelihood of the channel overestimation is not independent from the speed. As shown in Figure 3.16 the probability for an overestimation error rises drastic with the speed up to the point $v = 10$ m/s. Note, that here also the scenario-bounded goodput ratio starts to drop below one which means that the static scheme is more effective than the dynamic algorithm.

Also, the mean of the overestimation error illustrated in Figure 3.17 rises with the speed. Although in general this is the case for both assignment schemes and all modulation types, it does not equally affect the dynamic and the static case. Since higher modulation types are scheduled more often with the dynamic algorithm the overestimation error has a stronger influence to the SEP. Thus, if the maximum WT speed rises the increase in value and probability of occurrence of the overestimation error for the higher modulation types results in the drastic goodput decrease for dynamic scheduling as illustrated by the goodput ratios.

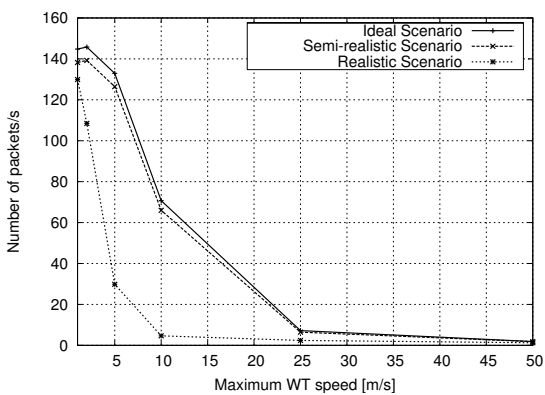


(a) Dynamic Algorithm

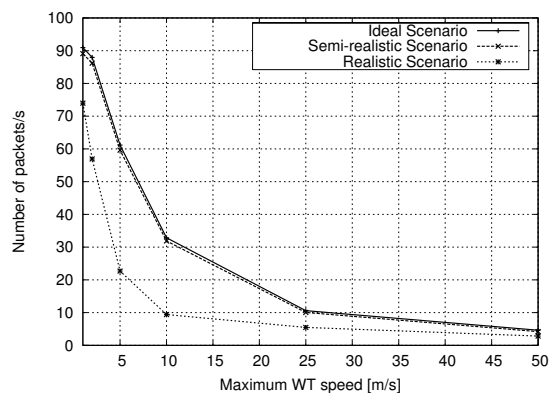


(b) Static Scheme

Figure 3.11: Absolute throughput of the dynamic and the static scheme for all scenarios with an increasing maximum speed of the Wireless Terminals in the cell

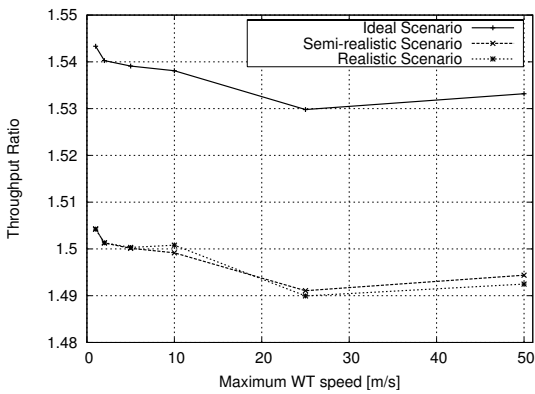


(a) Dynamic Algorithm

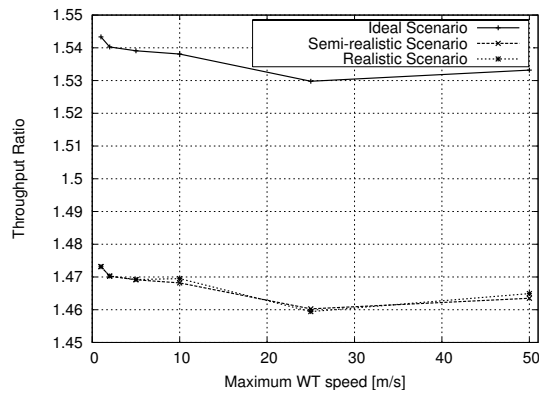


(b) Static Scheme

Figure 3.12: Absolute goodput of the dynamic and the static scheme for all scenarios with an increasing maximum speed of the Wireless Terminals in the cell

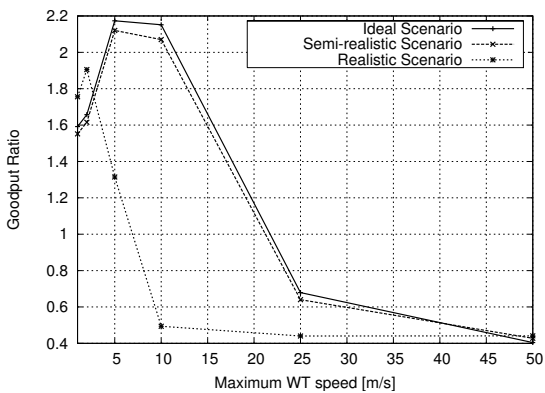


(a) Scenario-Bounded Ratio

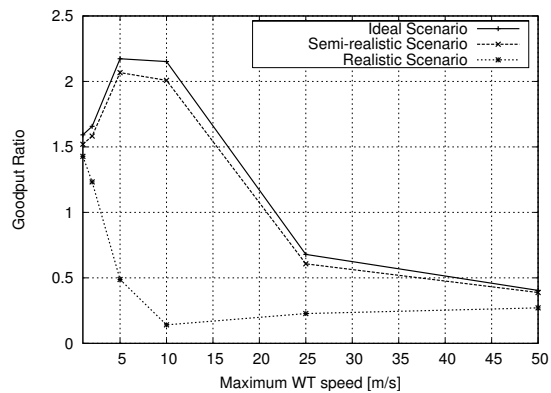


(b) Inter-Scenario Ratio

Figure 3.13: Throughput ratios for all scenarios with an increasing maximum speed of the Wireless Terminals in the cell



(a) Scenario-Bounded Ratio



(b) Inter-Scenario Ratio

Figure 3.14: Goodput ratios for all scenarios with an increasing maximum speed of the Wireless Terminals in the cell

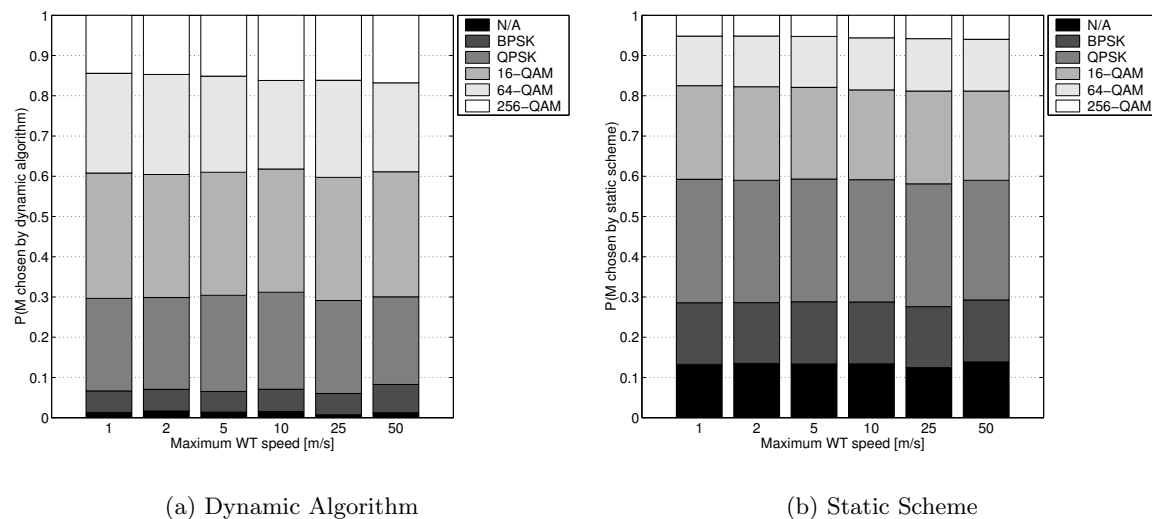


Figure 3.15: Probabilities for the assignment of a specific modulation type for the dynamic and the static scheme in the realistic scenario vs. an increasing maximum speed of the Wireless Terminals in the cell

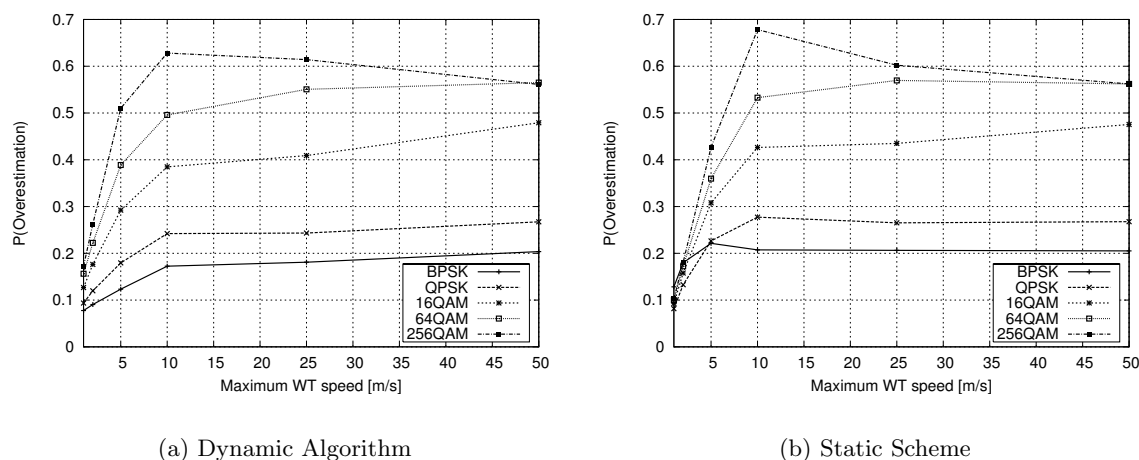


Figure 3.16: Probabilities for the overestimation of the channel state for the dynamic and the static scheme in the realistic scenario vs. an increasing maximum speed of the Wireless Terminals

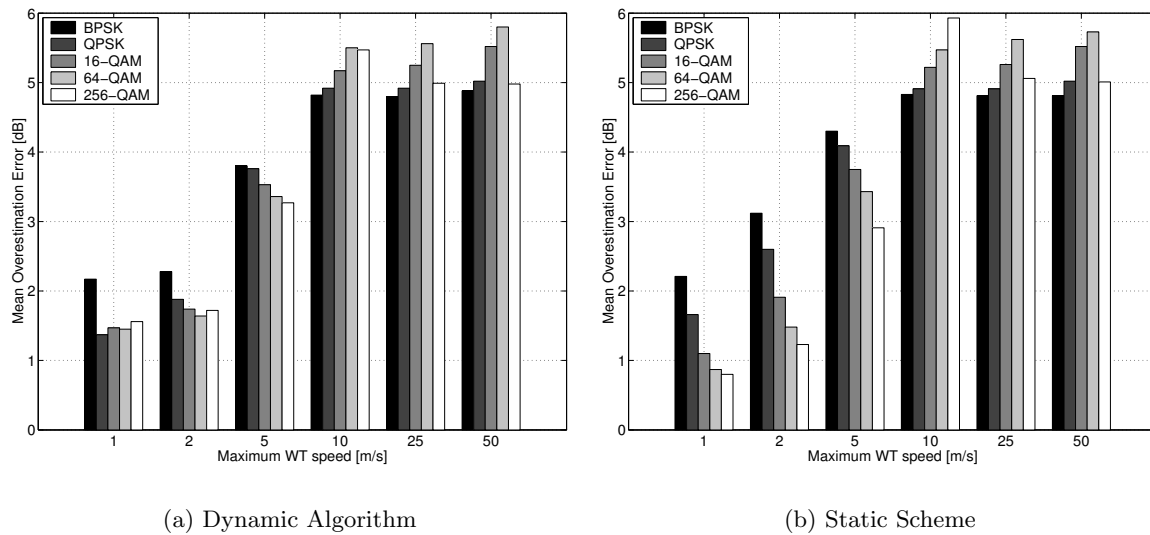


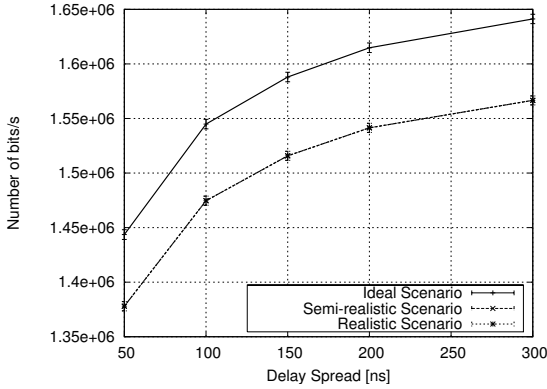
Figure 3.17: Mean values of the overestimation error for the dynamic and the static scheme in the realistic scenario vs. an increasing maximum speed of the Wireless Terminals

3.3.3 Varying the Delay Spread

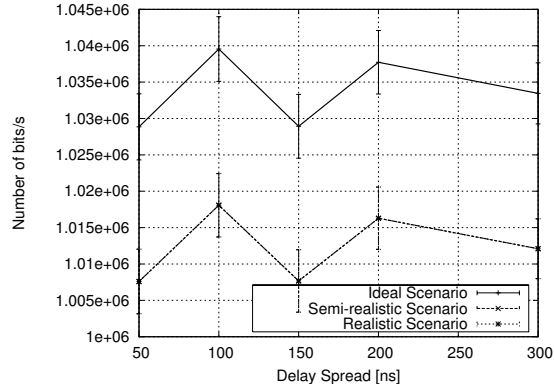
While the speed of the terminals is a parameter varying the time selective behavior of fading, the delay spread is the parameter varying the frequency selective behavior of the fading. Due to delay spread do different subcarriers have different channel gains for a certain fixed time and Wireless Terminal. The higher this spread is, the higher the gain difference is between two neighboring subcarriers (mathematically speaking, the higher the delay spread of the channel is the more uncorrelated do two neighboring subcarriers behave in terms of their attenuation). A good measure for the frequency selective behavior is the coherence bandwidth [10]. It gives a good frequency spacing measure for which subcarriers are still strongly correlated. In the here considered system subcarriers are spaced apart by 312.5 kHz. The following values were chosen for the delay spread: 50, 100, 150, 200, 300 ns. These delay spreads yield coherence bandwidth values of 3.2, 1.6, 1.0, 0.8, 0.5 MHz [1].

In Figures 3.18 and 3.19 the absolute values for the throughput and goodput results are shown for all three scenarios for the dynamic and the static scheme. Considering the absolute throughput values in terms of the static scheme with the shown confidence intervals (99% confidence level) there is generally no significant change for the varying delay spread. Merely a constant offset, caused by the added signaling information, is observable. Although this offset is also contained in the simulation results for the absolute throughput of the dynamic algorithm, here the behavior changes completely: Over an increasing delay spread the throughput increases significantly. Considering the chosen interval for the delay spread an increase of approximately 13.7% can be found. The strong difference between the behavior of the throughput values of the two schemes results from the fact that the static scheme is not able to benefit from the increase in frequency diversity caused by the increasing delay spread while the dynamic algorithm is able to adapt itself and therefore can take full advantage of this scenario change. Focusing on the goodput metric the described behavior is still present however here also the influence of the realistic subcarrier gain information can be observed. Considering the dynamic algorithm, the goodput values for all scenarios increase with the values for the delay spread, while the values for the realistic scenario are lowered by a nearly constant offset to the other two scenarios. As in the throughput metric the signaling adds a certain cost to our system, which lowers the curves for the semi-realistic and the realistic case. The influence of the realistic subcarrier gain information gets even stronger with the static scheme. Here the values for the realistic scenario are approximately 20.4% lower than for the semi-realistic case, while the curve slopes slightly for the realistic scenario.

In Figure 3.21(a) this effect turns out more clearly. The scenario-bounded ratio for the realistic scenario shows the completely different behavior of the two schemes: while with the dynamic algorithm the number of correctly received packets per second rises with the delay spread (Figure 3.19(a)) it slopes or at least stays flat with the static scheme (Figure 3.19(b)). This results in an strong increase of the scenario-bounded ratio for the realistic scenario from 1.47 to 1.89 for our chosen interval of $\Delta\sigma$. Note that the inter-scenario ratio compares the dynamic algorithm for all the three scenarios to the static scheme in an ideal scenario. In Figure 3.21(b) the influence of the added signaling data and the realistic subcarrier gain information is observable. In comparison to the inter-scenario ratio for the ideal scenario the signaling overhead lowers the ratio of the semi-realistic by approximately 4.7% while the goodput loss due to the realistic subcarrier gain information causes an additional offset

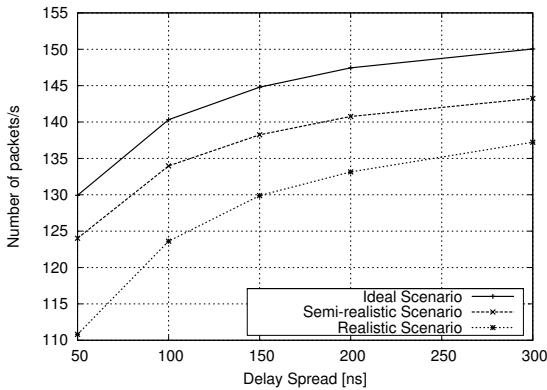


(a) Dynamic Algorithm

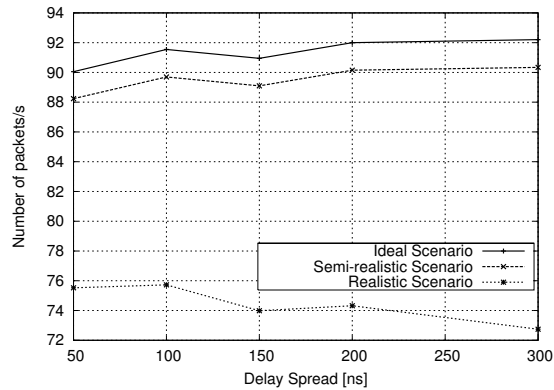


(b) Static Scheme

Figure 3.18: Absolute throughput of the dynamic and the static scheme for all scenarios with an increasing delay spread $\Delta\sigma$ in the cell



(a) Dynamic Algorithm

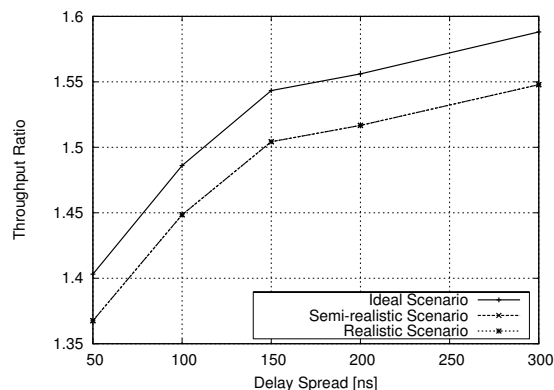


(b) Static Scheme

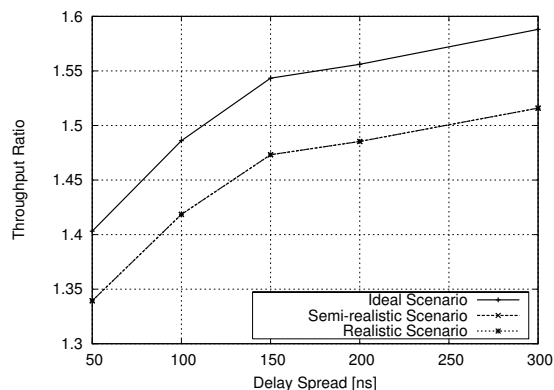
Figure 3.19: Absolute goodput of the dynamic and the static scheme for all scenarios with an increasing delay spread $\Delta\sigma$ in the cell

of approximately 6.4% to the inter-scenario ratio for the realistic scenario. Basically the qualitative behavior of the two throughput ratios, which are shown in Figure 3.20, is the same: Due to the fact that the absolute throughput rises with the dynamic algorithm while it stays flat with the static scheme, the ratios increase together with the values for the delay spread. Apart from the offset caused by the signaling data there is no significant difference between the simulation results of the three scenarios, since, as described in Section 3.3.1, realistic subcarrier gain information does not affect the throughput.

Figure 3.22 shows that with the dynamic algorithm the probability of choosing higher modulation types is much larger than with the static scheme, which explains the offset shown for the throughput ratios. The ratio for the QAM types illustrated in Figure 3.23 is always

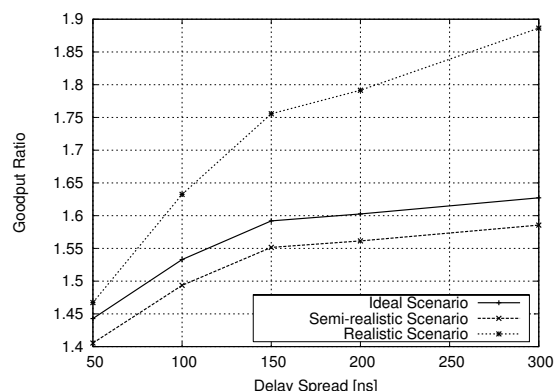


(a) Scenario-Bounded Ratio

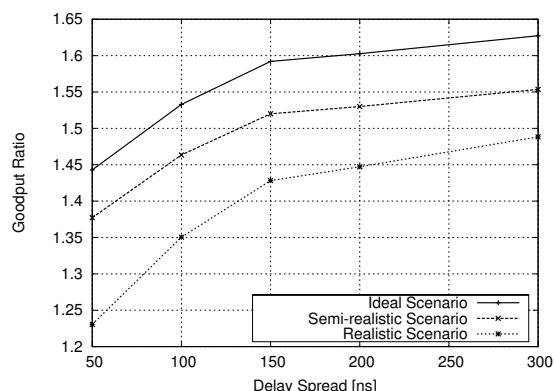


(b) Inter-Scenario Ratio

Figure 3.20: Throughput ratios for all scenarios with an increasing delay spread $\Delta\sigma$ in the cell



(a) Scenario-Bounded Ratio



(b) Inter-Scenario Ratio

Figure 3.21: Goodput ratios for all scenarios with an increasing delay spread $\Delta\sigma$ in the cell

higher than one and increases with the delay spread, which means that with the dynamic algorithm and rising $\Delta\sigma$ it becomes more and more likely to schedule QAM. Therefore, the benefit of the dynamic scheme, that is shown in both throughput ratios, rises with the delay spread, due to an increase in subcarrier state diversity.

While for rising $\Delta\sigma$ no significant change is shown for the occurrence and the mean of the overestimation error in the static case (Figure 3.24(b) and 3.25(b)), a slight increase shows up for the dynamic algorithm. Although the probability of an overestimation error is higher for larger modulation types (Figure 3.24(a)) and the rising mean for those modulation types typically affects the dynamic algorithm more drastic than the static scheme, this slight increase does not influence the goodput ratios since it is quite low in absolute numbers (below 2 dB in most cases).

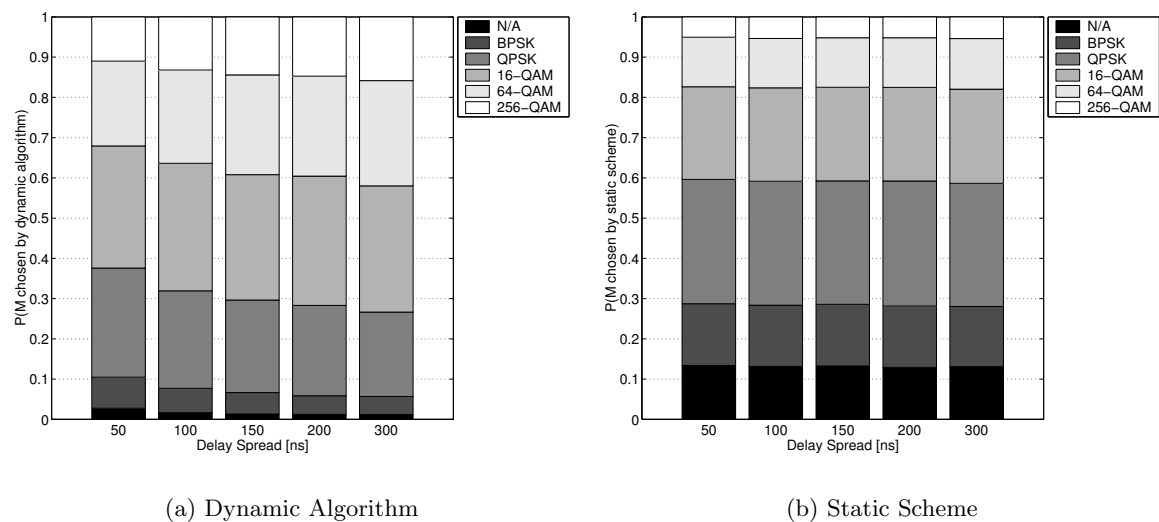


Figure 3.22: Probabilities for the assignment of a specific modulation type for the dynamic and the static scheme in the realistic scenario vs. an increasing delay spread $\Delta\sigma$

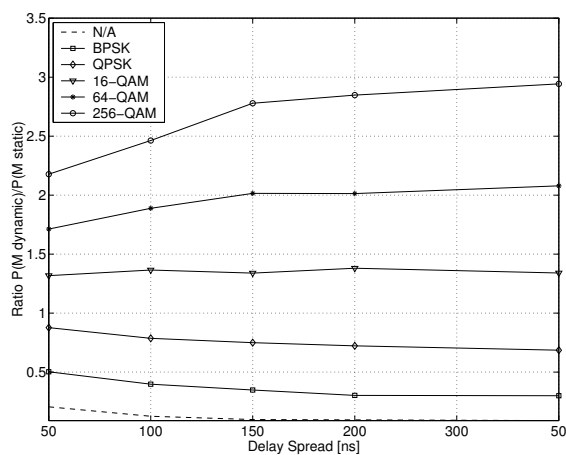
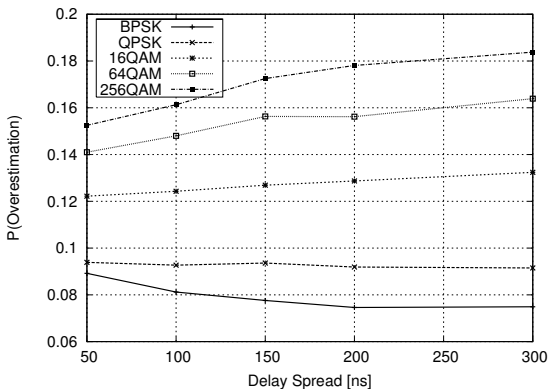
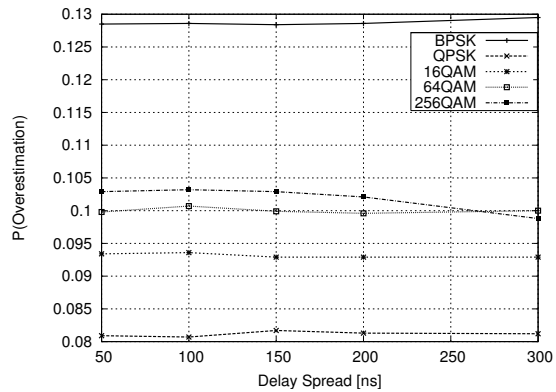


Figure 3.23: Comparison of the assignment probabilities of the dynamic vs. the static scheme in the realistic scenario for an increasing delay spread $\Delta\sigma$

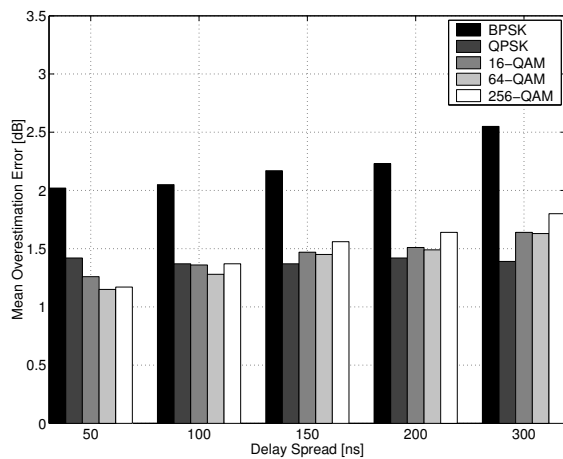


(a) Dynamic Algorithm

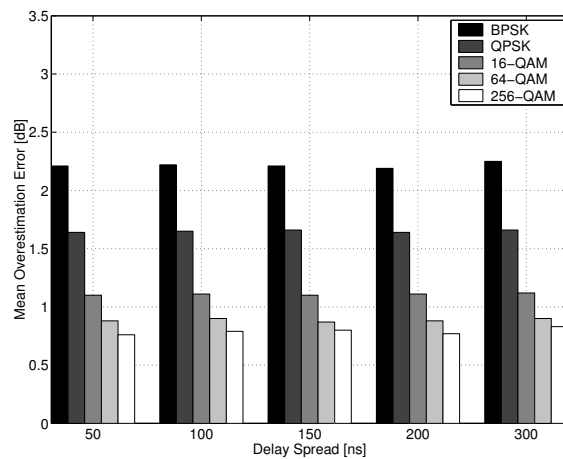


(b) Static Scheme

Figure 3.24: Probabilities for the overestimation of the channel state for the dynamic and the static scheme in the realistic scenario vs. an increasing delay spread $\Delta\sigma$



(a) Dynamic Algorithm



(b) Static Scheme

Figure 3.25: Mean values of the overestimation error for the dynamic and the static scheme in the realistic scenario vs. an increasing delay spread $\Delta\sigma$

3.3.4 Varying the Transmission Power

So far we used a constant value for the transmission power in our simulations which is derived from the IEEE 802.11a standard. The standard suggests a transmission power of -7 dBm per subcarrier for systems employing the frequency band around 5.2 GHz. However, for different frequency bands IEEE defined different maximum power values where the highest one is 800 mW for the complete frequency band at 5.8 GHz. In order to study the influence of the transmission power we varied it from -16 dBm up to 3 dBm.

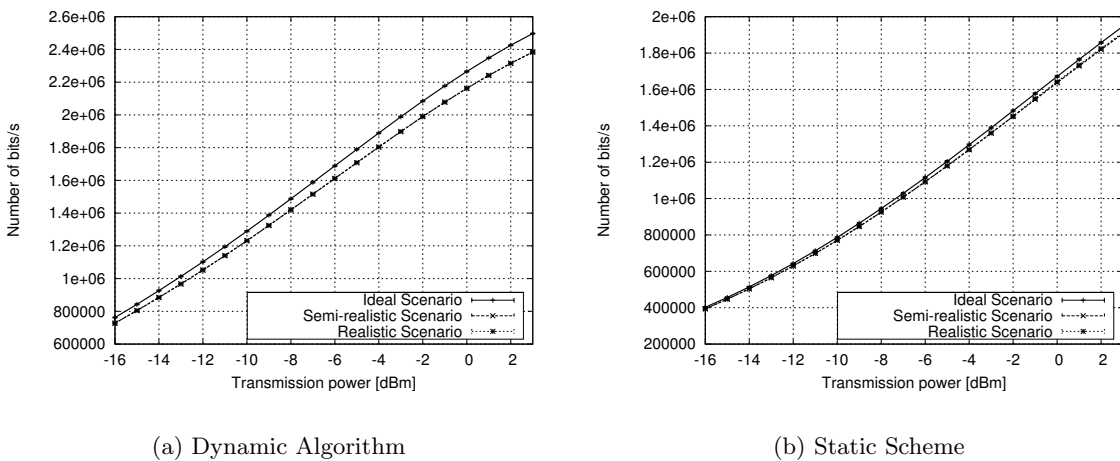


Figure 3.26: Absolute throughput of the dynamic and the static scheme for all scenarios with an increasing transmission power per subcarrier

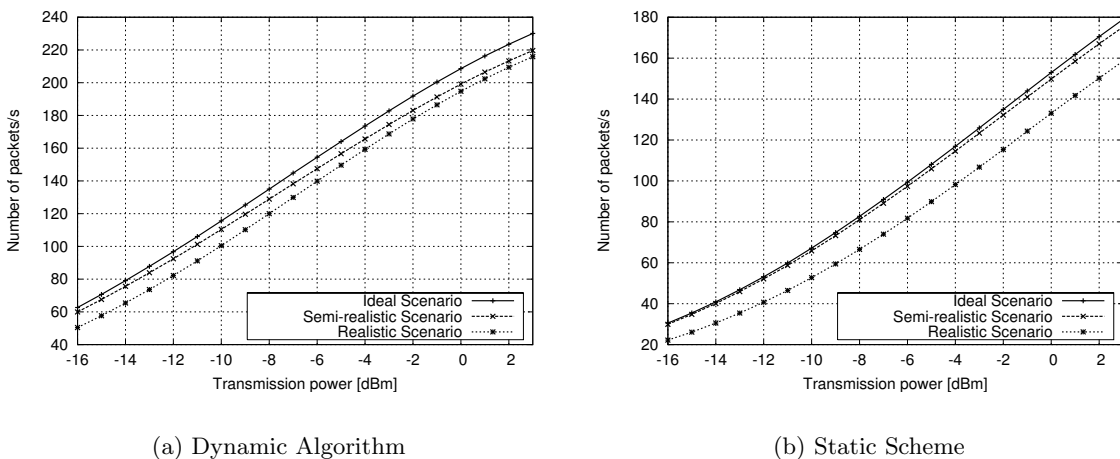


Figure 3.27: Absolute goodput of the dynamic and the static scheme for all scenarios with an increasing transmission power per subcarrier

In Figures 3.26 and 3.27 the absolute values for the throughput and goodput of the dynamic and static scheme are shown for the three different scenarios while varying the

transmission power. In general a higher transmission power will lead to higher SNR values per subcarrier. This allows the usage of modulation types with a higher data rate (e.g. 256-QAM instead of 16-QAM)). For both schemes the qualitative behavior of the absolute values for goodput and throughput is an increase with rising transmission power values. Comparing the simulation results for the throughput metric obtained with the static scheme to those of the dynamic algorithm a difference in the qualitative and quantitative behavior shows up. For rising transmission power values the number of transmitted bits per second obtained with the dynamic algorithm rises slower as with the static scheme, however it is much higher with the dynamic algorithm. Again, due to signaling overhead, an offset can be observed for both schemes, while the realistic subcarrier gain information has no effect to the throughput results. In the results for the absolute goodput, a similarity to the qualitative behavior of the results for the absolute throughput can be observed. However, the realistic subcarrier gain information causes an additional negative offset to the simulation results for the realistic scenario, due to the transmission errors which occur by using outdated channel knowledge for the subcarrier assignment.

This can be discussed more detailed with the goodput ratios presented in Figure 3.29. Comparing both schemes within one single scenario in the scenario-bounded ratio illustrates the mentioned qualitative behavior: While with the static scheme the number of correctly received packets rises very strong with rising values for P_{tx} it has a slightly logarithmic shape with the dynamic algorithm. This is due to the fact that with rising power values the states of the subbands are more likely to be good which reduces the opportunity of the dynamic algorithm to find few good subbands out of a large set of bad ones and assign them to the appropriate Wireless Terminals. Therefore the gain achieved by using the dynamic algorithm instead of the static scheme, which directly benefits from the improved subband states, is smaller. This results into a sloping scenario-bounded ratio for all the considered scenarios. Comparing the scenarios with the scenario-bounded ratio shows that the performance gain of the dynamic algorithm is much higher in the realistic scenario. This can be derived from the absolute goodput vales shown in Figure 3.27 where the negative offset caused by the realistic subcarrier gain information is much higher with the static scheme. Compared to the semi-realistic scenario this lasts to an performance gain up to approximately 13.2% if we take realistic subcarrier gain information into account. Since the signaling overhead is higher in case of the advanced algorithm this lowers the scenario-bounded ratio curve for the semi-realistic and the realistic scenario for approximately 2.6% in comparison to the ideal scenario. The realistic subcarrier gain information has also a drastic influence to the behavior of the curves for the inter-scenario ratio. While signaling causes a constant negative shift of approximately 4.7% to the results obtained with the semi-realistic scenario in comparison to the ideal scenario, the ratio for the realistic scenario shows a different behavior. Its linear decrease is not as steep as the slightly exponential decrease of the ratios for the other two scenarios but the difference between those curves is much higher for low values of P_{tx} than for high transmission power values. Considering our chosen interval of P_{tx} it varies from approximately 37.6% for -16 dBm to 1.7% for 3 dBm in comparison with the semi-realistic scenario. Since the probability that more subbands are in bad states rises with lower transmission power values, these results imply that the channel knowledge becomes more important as lower the transmission power is. Both throughput ratios, presented in Figure 3.28, show an slightly exponential decrease for all three scenarios. Since there is no

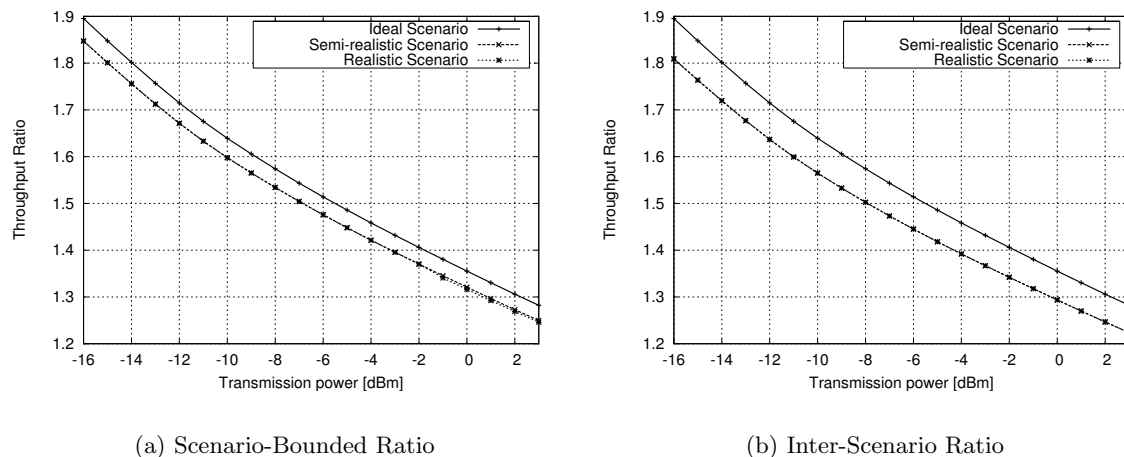


Figure 3.28: Throughput ratios for all scenarios with an increasing transmission power per subcarrier

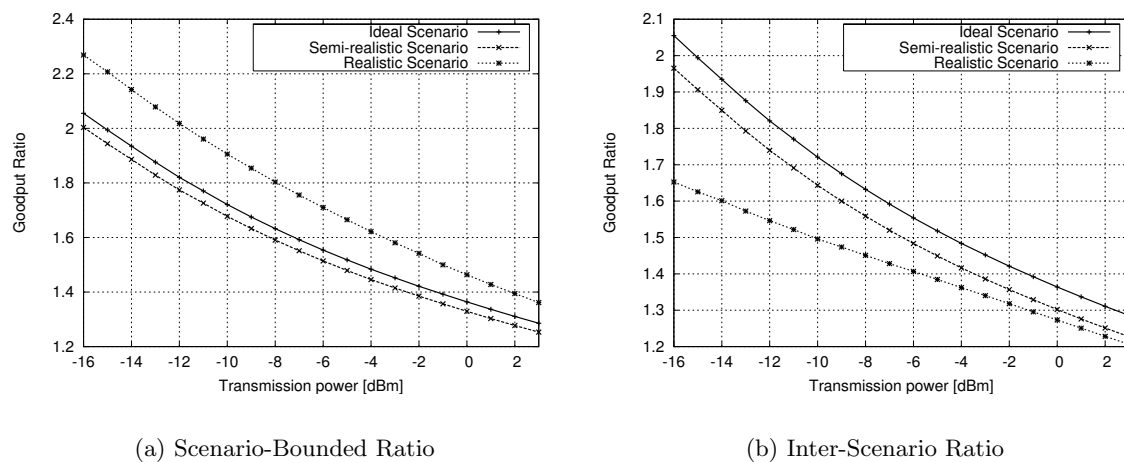


Figure 3.29: Goodput ratios for all scenarios with an increasing transmission power per subcarrier

influence of realistic subcarrier gain information they show the same qualitative behavior as the ideal and semi-realistic scenario for the goodput ratios. Signaling causes an offset of approximately 2.6% to the values for the semi-realistic and realistic scenario in the scenario-bounded ratio and 4.76% in the inter-scenario ratio.

For rising transmission power per subcarrier the probabilities for the assignment of a specific modulation type shown in Figure 3.30 change drastically. Due to the rising SNR for all subcarriers with rising transmission power higher modulation types are much more likely to be scheduled for both assignment schemes. However, as indicated by the throughput ratios, the dynamic algorithm performs better than the static scheme. Considering for example 256-QAM for the highest simulated transmission power shows, that the assignment probability is

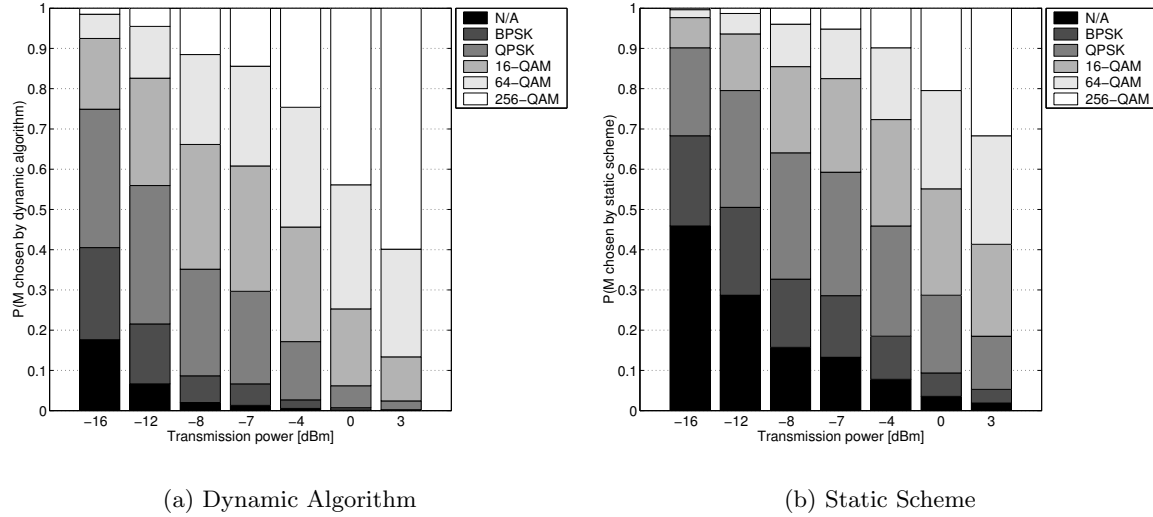


Figure 3.30: Probabilities for the assignment of a specific modulation type for the dynamic and the static scheme in the realistic scenario vs. an increasing transmission power per subcarrier

28% higher with the dynamic than with the static scheme.

As shown in general the SNR improvement leads to rising assignment probabilities for the higher modulation types. Although the dynamic scheduling makes better use of this improvement this is beneficial for both scheduling schemes. However, this improvement does not equally affect the dynamic and the static scheme. As illustrated in Figure 3.31 the gain achieved with the dynamic algorithm in comparison to the static scheme decreases with rising transmission power. Due to the overall improved subcarrier states the static assignment of subcarriers becomes more and more beneficial, while the dynamic scheme can not further improve by exploiting even higher modulation types (introducing a 1024 QAM modulation type would certainly change this situation again). In addition to the ratio for assignment probabilities this aspect is clearly represented by the decreasing throughput ratios in Figure 3.27(b).

For the further investigation of the goodput ratios the probability and mean of the overestimation error is given separately for each chosen modulation type in Figure 3.32 and 3.33. While for the dynamic algorithm a clear beneficial behavior is shown for higher transmission power, i.e. probability and the mean value of the overestimation error decrease for all modulation types, the results for the static case are different. Here the probability of an overestimation error increases for the lowest scheduled modulation type (BPSK) and decreases for all other modulation types. However, for high transmission power values this does not affect the goodput significantly since here the probability of choosing a lower modulation such as BPSK is relatively low. For the highest considered modulation type (256-QAM) the behavior is antagonistic: after an increase to $P_{tx} = -12$ dBm it strongly decreases for scenarios with higher transmission power.

In case of static subcarrier assignment the results for the mean of the overestimation error clearly rise for higher transmission power. As shown for the assignment probabilities

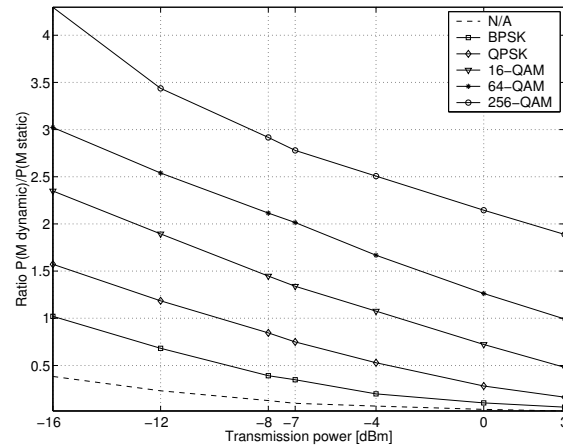
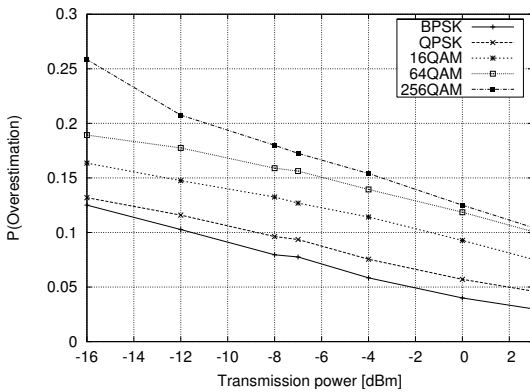
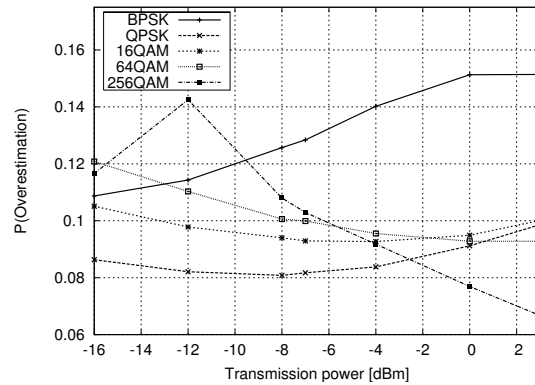


Figure 3.31: Comparison of the assignment probabilities of the dynamic vs. the static scheme in the realistic scenario for an increasing transmission power per subcarrier

for scenarios with lower transmission power the lower modulation types are chosen more often. Therefore, the mean overestimation error of the low modulation types, which is significantly higher in the dynamic case, has more influence in scenarios with lower transmission power. This explains the low inter-scenario goodput ratio for the realistic case in this range compared to the rate for the ideal and the semi-realistic scenario. Due to the benefits in SNR for all subcarriers for rising P_{tx} both assignment schemes profit in terms of goodput. However, the dynamic algorithm makes better use of the improved channel states (Figure 3.30) and does not suffer by rising mean values for the overestimation error (Figure 3.33), which explains the goodput ratio results greater than one.

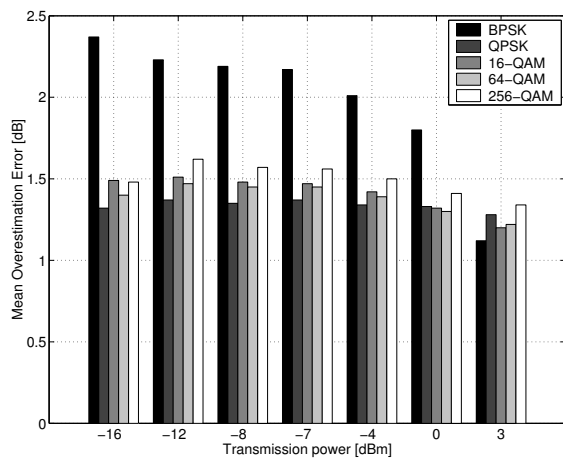


(a) Dynamic Algorithm

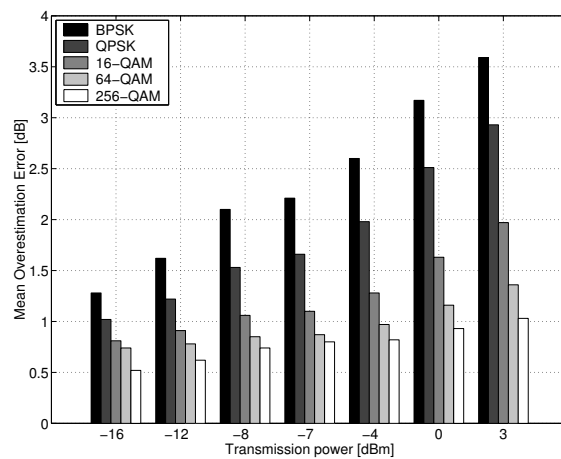


(b) Static Scheme

Figure 3.32: Probabilities for the overestimation of the channel state for the dynamic and the static scheme in the realistic scenario vs. an increasing transmission power per subcarrier



(a) Dynamic Algorithm



(b) Static Scheme

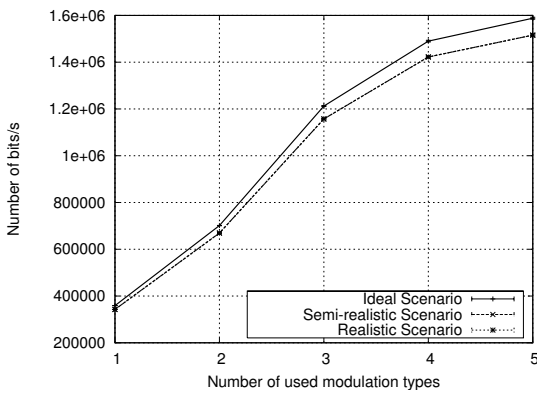
Figure 3.33: Mean values of the overestimation error for the dynamic and the static scheme in the realistic scenario vs. an increasing transmission power per subcarrier

3.3.5 Varying the Number of Used Modulation Types

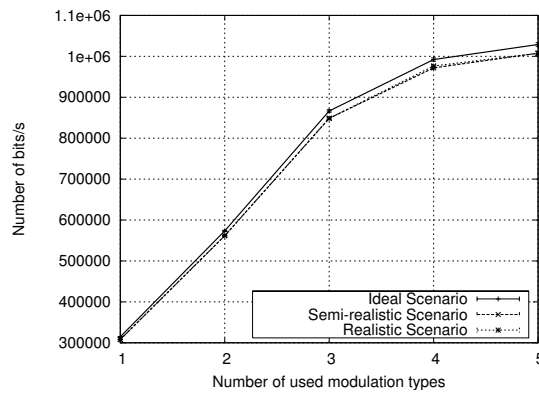
Two dimensions of adaption exist within the considered system. At first subcarriers can be assigned to different terminals which is done by dynamic assignment algorithms. Secondly, different modulation types might be used on these subcarriers. This form of adaption has been investigated in research much under the name of bit loading algorithms [7]. In this study we have applied a simple form of bit loading, a modulation type is always used if there is none with a higher bit rate which can achieve a certain maximum symbol error probability. Here we varied the number of modulation types used from one (BPSK only) to five (BPSK, QPSK, 16-QAM, 64-QAM, 256-QAM). Using only one modulation type equals the situation of the binary state wireless channel model from [5].

In general the absolute results obtained via simulation, presented in Figures 3.34 and 3.35, show the same behavior: The throughput and goodput results are rising with the number of modulation types, since, obviously, with a greater number of modulation types those types with higher bit rates can be used with adequate subcarrier states. As always signaling causes a slightly offset to the throughput and goodput values and with goodput the realistic scenario loses approximately 11% with the dynamic algorithm and approximately 24.4% with the static scheme due to realistic subcarrier gain knowledge. In terms of throughput the dynamic algorithm clearly outperforms the static scheme, however with goodput there is only a slight gain for a low number of used modulation types. For a higher number of modulation types available the gain is higher though. Note that the loss in terms of absolute goodput for both schemes in the case of realistic channel knowledge is quite constant and is therefore not influenced by how many modulation types are available.

Observing the scenario-bounded goodput ratio in Figure 3.37(a) the gain achieved by the dynamic algorithm can be examined for various amounts of modulation types. Here the performance gain, in terms of goodput, rises with higher numbers of M . Again, comparing the ideal and the semi-realistic scenario, the signaling offset shows up. The values obtained for the scenario-bounded goodput ratio in the realistic scenario show an interesting behavior: While for values of M smaller than 3 this ratio does not achieve the ratio values for the ideal scenario (note that the ratio value for $M = 1$ stands for an performance loss of approximately 4.2% comparing the dynamic algorithm to the static scheme), the ratio exceeds this bound for $M \geq 3$. This not only shows again the strong influence of taking realistic subcarrier gain information into account, it also leads to the conclusion that the dynamic algorithm, in comparison to the static scheme, performs even better with the problems caused by the lack of channel knowledge if the set of possible assignments, also represented by the amount of modulation types, is great enough. The influence of realistic subcarrier gain information is given in Figure 3.37(b). Considering this inter-scenario ratio for the realistic scenario leads to the fact that for $M < 3$ the goodput results obtained with the dynamic algorithm do not reach the results obtained with the static algorithm in the ideal scenario. For $M \geq 3$ a benefit is shown which rises logarithmic with M . The qualitative behavior of the throughput ratios, presented in Figure 3.36, is comparable to the behavior of the goodput ratios for the ideal and semi-realistic scenario. From $M = 2$ a logarithmic shape is observable, and again, a constant offset due to signaling has to be taken into account.

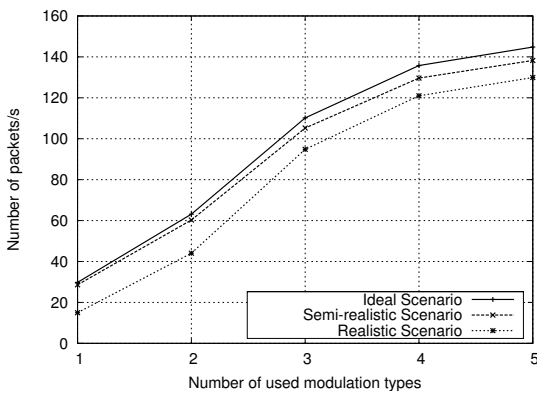


(a) Dynamic Algorithm

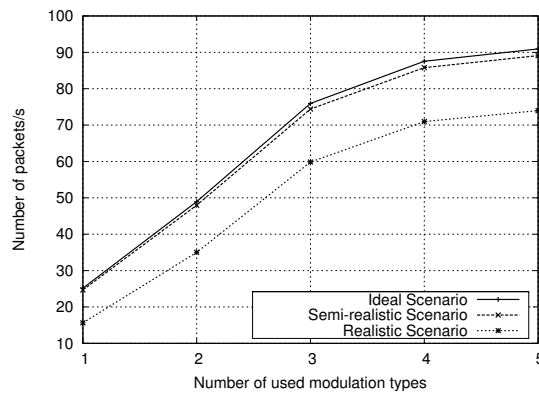


(b) Static Scheme

Figure 3.34: Absolute throughput of the dynamic and the static scheme for all scenarios with an increasing number of modulation types

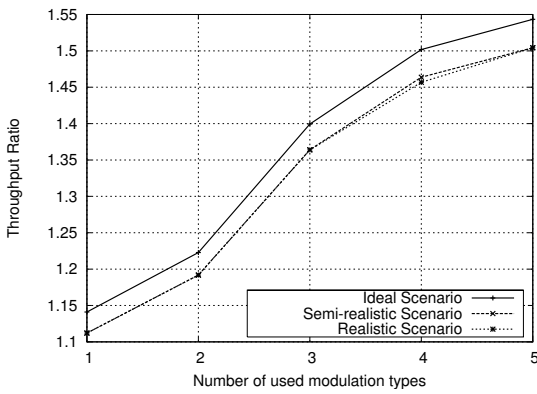


(a) Dynamic Algorithm

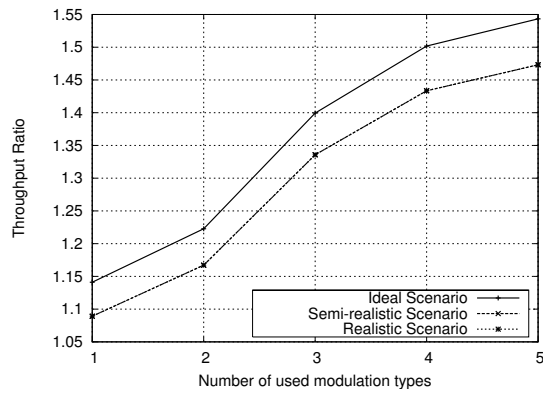


(b) Static Scheme

Figure 3.35: Absolute goodput of the dynamic and the static scheme for all scenarios with an increasing number of modulation types

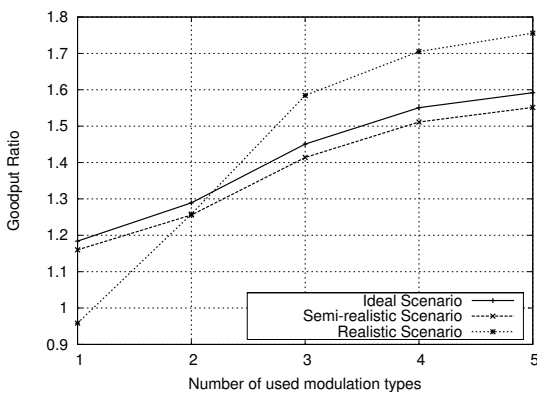


(a) Scenario-Bounded Ratio

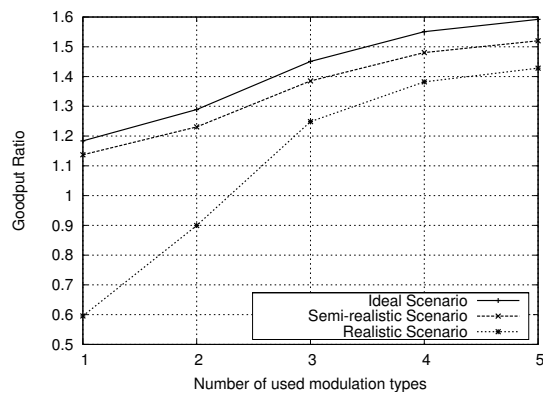


(b) Inter-Scenario Ratio

Figure 3.36: Throughput ratios for all scenarios with an increasing number of modulation types



(a) Scenario-Bounded Ratio



(b) Inter-Scenario Ratio

Figure 3.37: Goodput ratios for all scenarios with an increasing number of modulation types

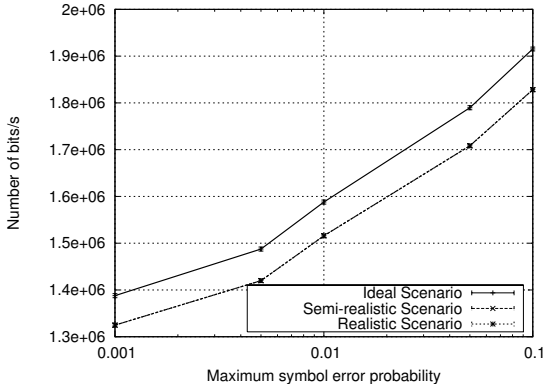
3.3.6 Varying the Maximum Symbol Error Probability

Considering the adaptive modulation system, beside the number of available modulation types also the maximum acceptable symbol error probability is an important parameter, influencing the performance of the adaptive system. By default it is set to 10^{-2} in this report. Note that the codes applied here have been chosen around the fact that the symbol error probability will be at a maximum at 10^{-2} . In this section we varied this probability from 10^{-3} up to 10^{-1} , while keeping the remaining system elements as they were, especially the the used block codes. This was done by varying the boundaries (channel state SNR values) which are used by both schemes to decide which modulation type is assigned to a certain subcarrier. E.g. if we want to rise P_s we lower the boundaries for all modulation types, which results into the usage of higher modulation types then appropriate and therefore into higher amounts of throughput and errors (also consider the SNR ranges of Figure 2.4).

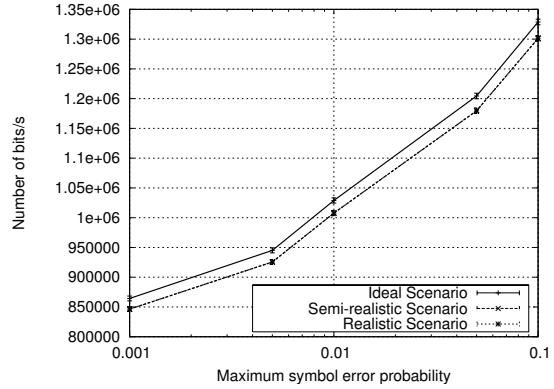
In Figures 3.38 and 3.39 the absolute throughput and goodput behavior is given for the dynamic and the static scheme in all three scenarios for a varying upper Symbol Error Probability (SEP) (logarithmic scaling of the x-axis). While, due to the fact that we assign higher modulation types to the subcarriers in order to achieve higher values of SEP, a steady throughput increase can be observed for both schemes for higher SEP. This is not the case if we consider the goodput. For the goodput the throughput behavior matches up to the SEP of 10^{-2} , afterwards goodput decreases instead of increasing. This is due to the used forward error correction scheme (introduced in Section 2.3.2), which is dimensioned to handle a SEP of 10^{-2} . It might also be used for a slightly higher value of SEP, but afterwards it can not protect transmissions from more often error occurrences.

This effect also shows up in the goodput ratios given in Figure 3.41. The ratios for all scenarios stay almost constant up to a SEP of 10^{-2} . After that point error coding becomes more and more unreliable and the ratio decreases significantly. The scenario bounded ratio shows a significant difference between the realistic and the two other scenarios. Until the above mentioned dropping point is reached the scenario-bounded ratio values for the realistic scenario are approximately 13.2% higher than for the semi-realistic scenario. Then it drops much stronger than for the scenarios without realistic subcarrier gain knowledge until it reaches a value of 0.87 for $P_s = 10^{-1}$. This shows two aspects of the dynamic algorithm under realistic conditions: First the gain achieved by the dynamic algorithm and second its sensitivity to errors and therefore the relevance of a appropriate error correction scheme. The inter-scenario ratio emphasizes this. After $P_s = 10^{-2}$ the ratio for realistic scenario drops with a higher slope than the ratio for the other two scenarios. In addition to the negative offset caused by the lack of channel knowledge, an offset caused by the signaling system is observable.

In Figure 3.40 the ratios of average throughput per terminal are given for different scenarios. In both Figures the ratio decreases constantly, which is due to the same phenomenon observed in the case of increasing the power, described in Section 3.3.4: If the maximum symbol error probability is increased, subcarriers are more likely to be in the best or at least in a good state, which reduces the possibilities for dynamic subcarrier assignment to find quite good subcarriers even if the the majority of the subcarriers is in a bad state. Due to this, for better subcarrier states the dynamic algorithm scales not as much as the static scheme and hence the ratio decreases. Adding the signaling system takes off the usual portion. In both

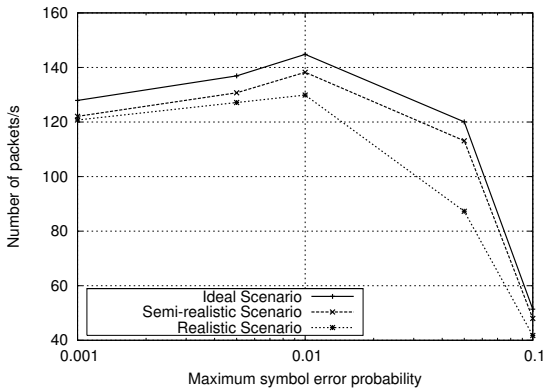


(a) Dynamic Algorithm

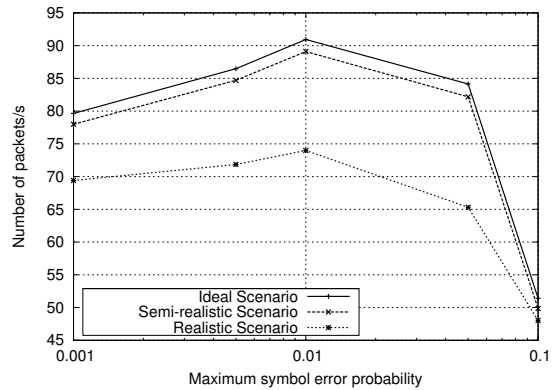


(b) Static Scheme

Figure 3.38: Absolute throughput of the dynamic and the static scheme for all scenarios with an increasing symbol error probability P_s



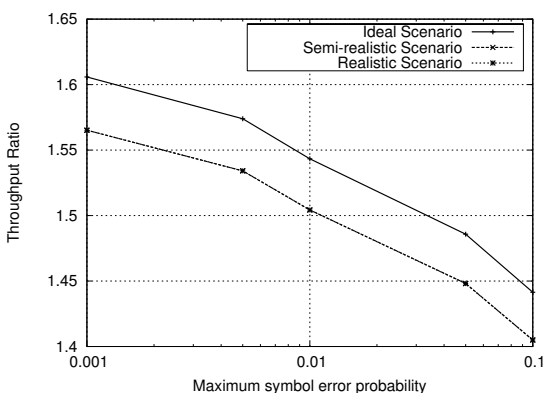
(a) Dynamic Algorithm



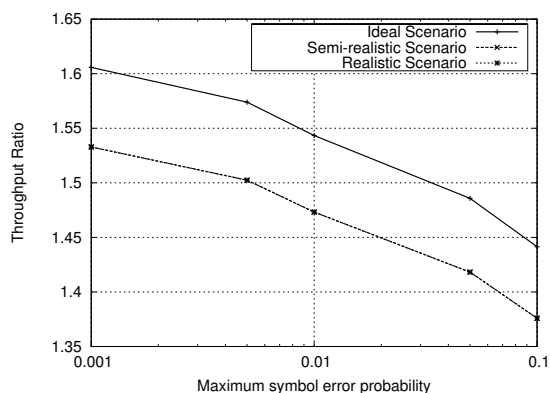
(b) Static Scheme

Figure 3.39: Absolute goodput of the dynamic and the static scheme for all scenarios with an increasing symbol error probability P_s

ratios there is no qualitative behavior change.

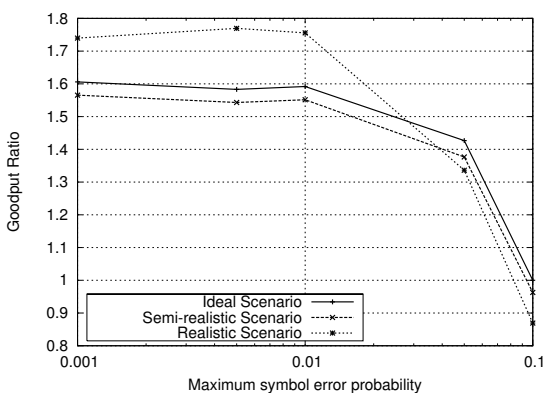


(a) Scenario-Bounded Ratio

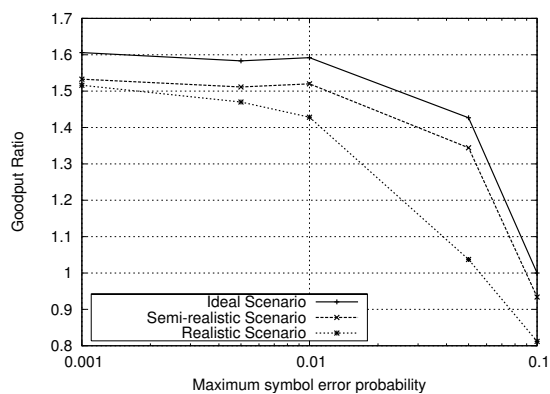


(b) Inter-Scenario Ratio

Figure 3.40: Throughput ratios for all scenarios with an increasing symbol error probability P_s



(a) Scenario-Bounded Ratio



(b) Inter-Scenario Ratio

Figure 3.41: Goodput ratios for all scenarios with an increasing symbol error probability P_s

Chapter 4

Conclusions

In this report we studied how the requirements of an existing signaling system and channel gain information feedback influences the downlink performance of a dynamic OFDM-FDMA system. In order to do so we used a simple MAC timing structure, which allows us to implement the required mechanisms and study their impact. We investigated average throughput and goodput performance of a dynamic and static subcarrier assignment algorithm under environments, as stated above, including the signaling and realistic channel knowledge, as well as both algorithms under an ideal environment without considering signaling and assuming perfect subcarrier knowledge. These studies were conducted under variation of various system parameters, such as the number of wireless terminals in the cell, different maximum speeds of the terminals, different delay spreads of the multipath environment, different transmission power levels per subcarrier, different maximum symbol error probabilities and different numbers of modulation types available.

Two questions have been given at the beginning of this report. First, if the lack of accurate and recent subcarrier attenuation knowledge might make the implementation of a dynamic OFDM-FDMA system impossible. This questions can be answered clearly, and the answer is that slightly outdated channel knowledge is not an obstacle which can not be overcome. Regarding channel knowledge it turns out that the speed of the wireless terminals is crucial to the systems performance. Up to a speed of running, the dynamic system design is beneficial compared to a static design. At faster speeds the performance of the dynamic system is more and more reduced. Note that the significance of the channel knowledge results relates strongly to the used coding scheme as well as to the used length of the downlink phase. Cutting the length of a MAC frame down to half the used time in this study, the dynamic system design probably can perform better for faster terminals (however, then the impact of signaling increases!). Beside the issue of speed it turns out in many cases that using a dynamic subcarrier assignment coupled with an adaptive modulation scheme is of more use than using only the adaptive modulation scheme, *especially* when it comes to realistic channel knowledge present at the access point. In these cases the static scheme suffers more from the realistic knowledge than the dynamic scheme, at least in terms of goodput. Therefore in general the fact that channel knowledge available at the access point is not perfect rather supports the idea of dynamic subcarrier scheduling than supporting the usage of a fixed TDMA or FDMA scheme. However, as mentioned prior, the fading rate is an issue of further study, since for fast fading rates this study shows that dynamic subcarrier scheduling is disadvantageous.

The second question studied in this report was the question for the impact of the additional overhead caused by dynamically scheduling subcarriers compared to only doing adaptive modulation without fixed subcarrier assignment. We find that using this kind of system setup, especially regarding the used frame length, the used bandwidth and the number of subcarriers this bandwidth is split up into, signaling is not a critical system component at all. On average the additional overhead caused by signaling is around 4 %, however the gain resulting from spending this overhead is around 50 % or above, such that the spending of this overhead turns out to be a good “investment”. No further drawbacks showed up during this study related to the usage of this signaling scheme.

As areas of further study we consider two important ones. Since this study unrevealed that the major bottleneck to overcome for dynamic OFDM-FDMA systems is the channel knowledge especially for faster terminal speed, new fields of activity mainly arise here. One question to answer here is if the usage of a different coding scheme such as convolutional codes changes the qualitative behavior of this system. Compared to block codes are convolutional codes related to a higher overhead, but also to a much better performance. This better performance could be beneficial for dynamic systems if the terminal speed is relatively high compared to indoor speeds. A second strategy is to highlight if there is the possibility to use the channel knowledge more effective. Of course the usage of a channel prediction unit is a very tempting option in this case. However, the complexity of such a combined system is definitely an issue. If channel prediction algorithms can use the realistically available channel information into more accurate one, this can be a major step towards implementing such a system. As third question, closely related to these previous ones, it is also possible to shorten the frame length. Of course there are multiple advantages but also disadvantages to this solution. So also regarding this question further investigation have to be conducted.

Appendix A

Acronyms

16-QAM 16 Quadrature Amplitude Modulation

64-QAM 64 Quadrature Amplitude Modulation

256-QAM 256 Quadrature Amplitude Modulation

ARQ Automatic Repeat Request

aDA advanced Dynamic Algorithm

AP Access Point

BCH Bose, Chaudhuri, and Hocquengham

BER Bit-Error-Rate

BPSK Binary Phase Shift Keying

BRAN Broadband Radio Access Networks

BS Base Station

CCITT International Consultative Committee on Telecommunications and Telegraphy

CNR Channel Gain-to-Noise Ratio

CRC Cyclic Redundancy Check

DL Downlink

DLC Data Link Control

DLPF Downlink Phase Frame

EFD End of the Frame Delimiter

FDM Frequency Division Multiplexing

FDMA Frequency Division Multiple Access

FEC Forward Error Correction
FSC Frame Check Sequence
ICI Intercarrier Interference
IEEE Institute of Electrical and Electronics Engineers, Inc.
ISI Intersymbol Interference
ISR Inter-Scenario Ratio
LAN Local Area Network
LLC Logical Link Control
MAC Medium Access Control
MCM Multi-Carrier Modulation
MTU Maximum Transmission Unit
OFDM Orthogonal Frequency Division Multiplexing
PDU Protocol Data Unit
PHY Physical
QPSK Quadrature Phase Shift Keying
RSSA Rotating Sub-Carrier Space Algorithm
SAF Sub-Band Assignment Field
SAM Sub-Band Assignment Matrix
SB Sub-Band
SBR Scenario-Bounded Ratio
SCM Single-Carrier Modulation
SEP Symbol Error Probability
SFD Start of the Frame Delimiter
SIG Signaling
SNR Signal-to-Noise Ratio
SNM SNR Matrix
sSA static Subcarrier Assignment

SSM Sub-band State Matrix

SYNC Synchronization

TDM Time Division Multiplexing

TDMA Time Division Multiple Access

UL Uplink

WT Wireless Terminal

WTs Wireless Terminals

Bibliography

- [1] A. Aguiar and J. Gross. Wireless channel models. Technical Report TKN-03-007, Telecommunication Networks Group, Technische Universität Berlin, April 2003.
- [2] J. Cavers. *Mobile Channel Characteristics*, chapter 1.3. Kluwer Academic, 2000.
- [3] ETSI. *Broadband Radio Access Networks (BRAN); HIPERLAN Type 2; Data Link Control (DLC) Layer; Part 1: Basic Data Transport Functions*, ts 101-761-1 edition, December 2001.
- [4] J. Gross. Dynamic scheduling of ofdm subcarriers for optimal support of cbr traffic in the down-link of a wireless cell. Master's thesis, Telecommunication Networks Group, Technische Universität Berlin, December 2001.
- [5] James Gross and Frank Fitzek. *Cannel State Dependent Scheduling Policies for an OFDM Physical Layer using a Binary State Model*. TKN Technical Report TKN-01-009. Telecommunication Networks Group, Berlin, 2001.
- [6] IEEE. *Supplement to Standard for Telecommunications and Information Exchange Between Systems - LAN/MAN Specific Requirements - Part 11: Wireless MAC and PHY Specifications: High Speed Physical Layer in the 5-GHz Band*, p802.11a/d7.0 edition, July 1999.
- [7] B. Krongold, K. Ramchandran, and D. Jones. Computationally efficient optimal power allocation algorithms for multicarrier communication systems. In *IEEE Int. Conference on Communications (ICC)*, pages 1018 – 1022, 1998.
- [8] Shu Lin and Jr. Daniel J. Costello. *Error Control Coding: Fundamentals and Applications*. Prentice-Hall, Inc., 1983.
- [9] Prof. Dr.-Ing. Peter Noll. *Nachrichtenübertragung II*. Skript zur Vorlesung TU Berlin, 2001.
- [10] J. Proakis. *Digital Communications*. McGraw-Hill, 1995.
- [11] T. Rappaport. *Wireless Communications Principles & Practice*. Prentice Hall PTR, Upper Saddle River, USA, 1999.
- [12] W. Rhee and J. Cioffi. Increase in capacity of multiuser ofdm sytem using dynamic subchannel allocation. In *Proc. Vehicular Technology Conference (VTC)*, pages 1085 – 1089, 2000.

- [13] William Stallings. *Data and Computer Communications*. Prentice-Hall, Inc., 6 edition, 2000.
- [14] A. Varga. *OMNET++ - Discrete Event Simulation System Documentation*. <http://whale.hit.bme.hu/omnetpp/>.
- [15] H. Yin and H. Liu. An efficient multiuser loading algorithm for ofdm-based broadband wireless systems. In *Proc. IEEE Globecom*, 2000.